Molecular Pharmacology Fast Forward. Published on May 29, 2009 as doi: 10.1124/mol.109.056523
This article has not been copyedited and formatted. The final version may differ from this version.

Sorafenib and Vorinostat kill colon cancer cells by CD95-dependent and –independent mechanisms.

Teneille Walker, Clint Mitchell, Margaret A. Park, Adly Yacoub, Martin Graf,

Mohamed Rahmani, Peter J. Houghton, Christina Voelkel-Johnson, Steven Grant, and Paul Dent*

Departments of Biochemistry (PD, TW, CM, MAP, SG), Medicine (SG, MR), Radiation Oncology (AY), Neurosurgery (MG), Institute for Molecular Medicine (PD, SG), Virginia Commonwealth University, 401 College St., Richmond, VA 23298; Medical University of South Carolina (CVJ), Department of Microbiology and Immunology, PO Box 250504/BSB201, 173 Ashley Avenue, Charleston, SC 29425; Department Molecular Pharmacology (PJH), St. Jude Children's Research Hospital, Memphis, TN 38105.

Molecular Pharmacology Fast Forward. Published on May 29, 2009 as DOI: 10.1124/mol.109.056523
This article has not been copyedited and formatted. The final version may differ from this version.

Running Title: HDACIs and Sorafenib.

Abbreviations: Vor.: Vorinostat; Sor.: Sorafenib; Val.: sodium valproate; ERK: extracellular regulated kinase; MEK: mitogen activated extracellular regulated kinase; EGF: epidermal growth factor; PARP: poly ADP ribosyl polymerase; PI3K: phosphatidyl inositol 3 kinase; -/-: null / gene deleted; ERK: extracellular regulated kinase; MAPK: mitogen activated protein kinase; MEK: mitogen activated extracellular regulated kinase; R: receptor; JNK: c-Jun NH_2-terminal kinase; dn: dominant negative; P: phospho-; ca: constitutively active; WT: wild type; ASMase: acidic sphingomyelinase; siSCR: siRNA scrambled control.

*Correspondence to:
Paul Dent, Ph.D.
Department of Biochemistry and Molecular Biology
401 College Street, Massey Cancer Center,
Room 280a, Box 980035
Virginia Commonwealth University
Richmond VA 23298-0035.
Tel: 804 628 0861
Fax: 804 827 1309
pdent@vcu.edu

Number of text pages: 36
Number of Tables: 4
Number of Figures: 6
Words in Abstract: 238
Words in Introduction: 723
Words in Discussion: 1521

Molecular Pharmacology Fast Forward. Published on May 29, 2009 as DOI: 10.1124/mol.109.056523
This article has not been copyedited and formatted. The final version may differ from this version.

Abstract.

We examined the interaction between the multi-kinase inhibitor sorafenib and histone deacetylase inhibitors. Sorafenib and vorinostat synergized to kill HCT116 and SW480 cells. In SW480 cells, sorafenib+ vorinostat increased CD95 plasma membrane levels and promoted DISC formation, and drug toxicity was blocked by knock down of CD95 or over-expression of c-FLIP-s. In SW620 cells that are patient matched to SW480 cells, sorafenib+vorinostat toxicity was significantly lower that correlated with a lack of CD95 activation and lower expression of ceramide synthase 6 (LASS6). Over-expression of LASS6 in SW620 cells enhanced drug-induced CD95 activation and enhanced tumor cell killing, whereas knock down of LASS6 in SW480 cells suppressed CD95 activation. Knocking down LASS6 expression also suppressed CD95 activation in hepatoma, pancreatic and ovarian cancer cells. In HCT116 cells sorafenib+vorinostat treatment caused DISC formation without reducing c-FLIP-s expression and did not increase CD95 plasma membrane levels; sorafenib+vorinostat exposure killed HCT116 cells via an intrinsic pathway / caspase 9-dependent mechanism. In HCT116 cells knock down of CD95 *enhanced* sorafenib+vorinostat lethality and that correlated with less drug-induced CD95-dependent autophagy. Sorafenib+vorinostat treatment activated the JNK pathway which was causal in promoting dissociation of Beclin1 from BCL-2, and in promoting autophagy. Knock down of Beclin1 expression blocked autophagy and enhanced drug toxicity. Our data demonstrate that treatment of colon cancer cells with sorafenib+vorinostat activates CD95 via de novo ceramide synthesis that promotes viability via autophagy or degrades survival via either the extrinsic or intrinsic pathways.

Molecular Pharmacology Fast Forward. Published on May 29, 2009 as DOI: 10.1124/mol.109.056523
This article has not been copyedited and formatted. The final version may differ from this version.

Introduction.

In the United States, colon cancer is diagnosed in ~150,000 patients peer annum with ~50,000 deaths from the disease, with a 5 year survival rate of ~60% (Parkin et al, 2002; Hedge et al, 2008). However, for patients with non-localized tumor at diagnosis, the 5 year survival is ~10%.

The Raf-MEK1/2-ERK1/2 pathway is frequently dysregulated in neoplastic transformation (Dent et al, 2003; Dent et al, 2005; Valerie et al, 2007). The MEK1/2-ERK1/2 module comprises, along with c-Jun NH_2-terminal kinase (JNK1/2) and p38 MAPK, members of the MAPK super-family. These kinases are involved in responses to diverse mitogens and environmental stresses and have also been implicated in cell survival processes. Activation of the ERK1/2 pathway is often associated with cell survival whereas JNK1/2 and p38 MAPK pathway signaling often causes apoptosis. Although the mechanisms by which ERK1/2 activation promote survival are not fully characterized, a number of anti-apoptotic effector proteins have been identified, including increased expression of anti-apoptotic proteins such as c-FLIP (Grant and Dent, 2006; Allan et al, 2003; Mori et al, 2003; Ley et al, 2003; Wang et al, 2007; Qiao et al, 2003). In view of the importance of the RAF-MEK1/2-ERK1/2 pathway in neoplastic cell survival, inhibitors have been developed that have entered clinical trials, including sorafenib (Bay 43-9006, Nexavar®; a Raf kinase inhibitor) and AZD6244 (a MEK1/2 inhibitor) (li et al, 2007; Davies et al, 2007).

Sorafenib is a multi-kinase inhibitor that was originally developed as an inhibitor of Raf-1, but which was subsequently shown to inhibit multiple other kinases, including class III tyrosine kinase receptors such as platelet-derived growth factor, vascular endothelial growth factor receptors 1 and 2, c-Kit and FLT3 (Flaherty, 2007). Anti-tumor effects of sorafenib in renal cell carcinoma and in hepatoma have been ascribed to anti-angiogenic actions of this agent through inhibition of the growth factor receptors (Rini, 2006; Srumberg, 2005; Gollob, 2005). Several groups, including ours, have shown *in vitro* that sorafenib kills human leukemia cells at concentrations below the maximum achievable dose (C_{max}) of 15-20 μM, through a mechanism involving down-

Molecular Pharmacology Fast Forward. Published on May 29, 2009 as DOI: 10.1124/mol.109.056523
This article has not been copyedited and formatted. The final version may differ from this version.

regulation of the anti-apoptotic BCL-2 family member MCL-1 (Rahmani et al, 2005; Rahmani et al, 2007a). In these studies sorafenib-mediated MCL-1 down-regulation occurred through a translational rather than a transcriptional or post-translational process that was mediated by endoplasmic reticulum (ER) stress signaling (Dasmahapatra et al., 2007; Rahmani et al, 2007b). This suggests that the previously observed anti-tumor effects of sorafenib are mediated by a combination of inhibition of *Raf* family kinases and the ERK1/2 pathway; receptor tyrosine kinases that signal angiogenesis; and the induction of ER stress signaling.

Histone deacetylase inhibitors (HDACI) represent a class of agents that act by blocking histone de-acetylation, thereby modifying chromatin structure and gene transcription. HDACs, along with histone acetyl-transferases, reciprocally regulate the acetylation status of the positively charged NH_2-terminal histone tails of nucleosomes. HDACIs promote histone acetylation and neutralization of positively charged lysine residues on histone tails, allowing chromatin to assume a more open conformation, which favors transcription (Gregory et al., 2001). However, HDACIs also induce acetylation of other non-histone targets, actions that may have plieotropic biological consequences, including inhibition of HSP90 function, induction of oxidative injury and up-regulation of death receptor expression (Marks et al., 2003; Bali et al., 2005; Kwon et al., 2002). With respect to combinatorial drug studies with a multi-kinase inhibitor such as sorafenib, HDACIs are of interest in that they have potential to down-regulate multiple oncogenic kinases by interfering with HSP90 function, leading to proteasomal degradation of these proteins. Vorinostat (suberoylanilide hydroxamic acid, SAHA, Zolinza®) is a hydroxamic acid HDACI that has shown preliminary pre-clinical evidence of activity in hepatoma and other malignancies with a C_{max} of ~9 μM (Pang and Poon, 2007; Venturelli et al, 2007; Wise et al, 2007).

We recently published that sorafenib and vorinostat interact to kill in renal, hepatocellular and pancreatic carcinoma cells via activation of the CD95 extrinsic apoptotic pathway, concomitant with drug-induced reduced expression of c-FLIP-s via PKR like endoplasmic reticulum kinase (PERK) signaling to eIF2α (Zhang et al, 2008; Park et al, 2008a). Subsequent work mechanistically advanced our understanding to reveal that sorafenib

Molecular Pharmacology Fast Forward. Published on May 29, 2009 as DOI: 10.1124/mol.109.056523
This article has not been copyedited and formatted. The final version may differ from this version.

and vorinostat interact by activating acidic sphingomyelinase and the de novo ceramide pathway to promote CD95 activation which regulates both apoptosis and autophagy. The present studies determined whether the same killing mechanisms apply after sorafenib and vorinostat treatment in colon cancer cells.

Molecular Pharmacology Fast Forward. Published on May 29, 2009 as DOI: 10.1124/mol.109.056523
This article has not been copyedited and formatted. The final version may differ from this version.

Materials and Methods.

Materials. The Vorinostat, Sorafenib, and Obatoclax used in this manuscript were generously provided by Merck and Co., Inc., Bayer Healthcare Pharmaceuticals, and Gemin X Biotechnologies, respectively, and the National Cancer Institute, NIH. Primary antibodies were purchased from Cell Signaling Technologies (Worcester, MA). HCT116, SW480, SW620, DLD1, PANC1, HEPG2, OVCAR and SKOVIII carcinoma cells were purchased from the ATCC. SW620 cells expressing LASS6 were provided by Dr. Voelkel-Johnson. Rh30 and Rh41 rhabdomyosarcoma cells were provided by Dr. Houghton. HCT116 parental cells that express K-RAS D13 and transfected with CMV empty vector; HCT116 cells deleted for the single allele of K-RAS D13; HCT116 cells deleted for K-RAS D13 stably expressing H-RAS V12 and also transfected with effector mutants of H-RAS V12 were as described in Ihle et al., 2009. Commercially available validated short hairpin RNA molecules to knock down RNA / protein levels were from Qiagen (Valencia, CA): CD95 (SI02654463; SI03118255); ATG5 (SI02655310); Beclin 1 (SI00055573, SI00055587). We also made use for confirmatory purposes of the short hairpin RNA construct targeting *ATG5* (pLVTHM/Atg5) that was a generous gift from Dr. Yousefi, Department of Pharmacology, University of Bern, Bern Switzerland. The plasmids to express green fluorescent protein (GFP)- tagged human LC3; wild type and dominant negative PERK (Myc-tagged PERKΔC); were kindly provided by Dr. S. Spiegel, VCU, Dr. J.A. Diehl University of Pennsylvania, Philadelphia, PA. Reagents and performance of experimental procedures were described in (Rahmani et al, 2007a; Rahmani et al, 2007b; Zhang et al, 2008; Park et al, 2008a; Park et al, 2008b; Park et al, 2008c; Yacoub et al, 2008; Mitchell et al, 2007; Qiao et al, 2001).

Methods.

Culture and in vitro exposure of cells to drugs. All established cell lines were cultured at 37 ^{o}C (5% (v/v CO_2) *in vitro* using RPMI supplemented with 5% (v/v) fetal calf serum and 10% (v/v) Non-essential amino acids. For short term cell killing assays, and immunoblotting studies, cells were plated at a density of 3 x 10^3 per cm^2 (~2 x 10^5 cells per well of a 12 well plate) and 48h after plating treated with various drugs, as indicated. *In vitro* vorinostat and sorafenib treatments were from 100 mM stock solutions of each drug and the maximal

Molecular Pharmacology Fast Forward. Published on May 29, 2009 as DOI: 10.1124/mol.109.056523
This article has not been copyedited and formatted. The final version may differ from this version.

concentration of Vehicle (DMSO) in media was 0.02% (v/v). Cells were not cultured in reduced serum media during any study in this manuscript. HCT116 (parental and transfected variants thereof), HEPG2, OVCAR, Rh30, Rh41 and SKOVIII cells were treated in all studies unless otherwise indicated with 3 μM sorafenib. PANC1, SW620, SW480 and DLD1 cells were treated in all studies unless otherwise indicated with 6 μM sorafenib. Unless otherwise indicated, cells were treated with 500 nM vorinostat and 1.0 mM sodium valproate. Unless otherwise indicated, cells were treated with 100 nM Obatoclax (GX15-070).

In vitro cell treatments, microscopy, SDS-PAGE and Western blot analysis. For in vitro analyses of short-term cell death effects, cells were treated with Vehicle or vorinostat or Na valproate / sorafenib for the indicated times in the Figure legends. For apoptosis assays where indicated, cells were pre-treated with vehicle (VEH, DMSO) and therapeutic drugs; cells were isolated at the indicated times, and either subjected to trypan blue cell viability assay by counting in a light microscope. Alternatively, the Annexin V/propidium iodide assay was carried to determine cell viability out as per the manufacturer's instructions (BD PharMingen) using a Becton Dickinson FACScan flow cytometer (Mansfield, MA).

For SDS PAGE and immunoblotting, cells after the indicated time of treatment, lysed in whole-cell lysis buffer (0.5 M Tris-HCl, pH 6.8, 2%SDS, 10% glycerol, 1% β-mercaptoethanol, 0.02% bromophenol blue), and the samples were boiled for 30 min. The boiled samples were loaded onto 10-14% SDS-PAGE and electrophoresis was run overnight. Proteins were electrophoretically transferred onto 0.22 μm nitrocellulose, and immunoblotted with various primary antibodies against different proteins. All immunoblots were visualized by an Odyssey Infra Red Imaging system. For presentation, immunoblots were digitally processed at 600 dpi using Adobe PhotoShop CS2, and their color removed and Figures generated in MicroSoft PowerPoint.

Infection of cells with recombinant adenoviruses. Cells were plated at 3 x 10^3 per cm^2 in each well of a 12 well, 6 well or 60 mm plate. After plating (24h), cells were infected (hepatoma and pancreatic carcinoma; at a

Molecular Pharmacology Fast Forward. Published on May 29, 2009 as DOI: 10.1124/mol.109.056523
This article has not been copyedited and formatted. The final version may differ from this version.

multiplicity of infection of 50) with a control empty vector virus (CMV) and adenoviruses to express MEK1 EE, caAKT, dnMEK1, dnAKT, CRM A, c-FLIP-s, BCL-XL, or XIAP (Vector Biolabs, Philadelphia, PA). After infection (24h) cells were treated with the indicated concentrations of vorinostat or Na valproate / sorafenib and/or other drugs, and cell survival or changes in expression / phosphorylation determined 0-96h after drug treatment.

Transfection of cells with siRNA or with plasmids. Transfection protocols were identical to those performed as described in Zhang et al, 2008; Park et al, 2008a, with siRNA transfection at 20 nM.

CD95 cell surface density measurement. Five random cells are selected from each treatment condition. The density of CD95 staining is measured at 50 points per cell under a fluorescent microscope using Axiocam / Axiovision imaging software.

Data analysis. Comparison of the effects of various treatments was performed using ANOVA and the Student's t test. Differences with a *p*-value of < 0.05 were considered statistically significant. Experiments shown are the means of multiple individual points (± SEM). Median dose effect isobologram analyses are a quantitative assessment to determine whether drug interactions were additive or synergistic. Synergy calculations were performed according to the Methods of T.-C. Chou and P. Talalay using the Calcusyn program for Windows (BIOSOFT, Cambridge, UK). A combination index (CI) value of less than 1.00 indicates synergy of interaction between the drugs; a value of 1.00 indicates additivity; a value of > 1.00 equates to antagonism of action between the agents.

Molecular Pharmacology Fast Forward. Published on May 29, 2009 as DOI: 10.1124/mol.109.056523
This article has not been copyedited and formatted. The final version may differ from this version.

Results.

In short term cell viability assays, sorafenib and vorinostat interacted in an additive to greater than additive manner to kill SW480, DLD-1 and HCT116 colon cancer cells (Figure 1A). Of note, while sorafenib and vorinostat interacted in a greater than additive manner to kill SW480 cells; patient matched SW620 cells were resistant to drug-induced lethality. HCT116 cells, and variants of HCT116 cells that are genetically deleted for K-RAS D13 and transfected with empty vector (CMV), H-RAS V12 or effector mutants of H-RAS V12 that activate specific downstream pathways, were next treated with sorafenib and vorinostat. The H-RAS V12 effector mutants selectively activate RAF (H-RAS V12-S35); RALGDS (H-RAS V12-G37); and PI3K (H-RAS V12-C40), respectively. Sorafenib and vorinostat toxicity was reduced in tumor cells lacking mutant active K-RAS D13 expression, was restored in cells expressing H-RAS V12 and was enhanced in tumor cells with H-RAS V12-dependent activation of ERK1/2, but not in cells with H-RAS V12 -dependent activation of either the PI3K or RALGDS signaling pathways (Figure 1B) (Martin et al, 2008; Ihle et al, 2008). In long-term colony formation assays sorafenib and vorinostat interacted in a synergistic manner to kill HCT116 and SW480 cells, as judged by combination index values of less than 1.00 (Table 1). Similar synergistic tumor cell killing / colony formation data were obtained when an unrelated clinically used HDACI, sodium valproate, was substituted for vorinostat (Table 2).

Prior studies have demonstrated in hepatoma and renal carcinoma cells that sorafenib+vorinostat toxicity was dependent on activation of CD95 (Zhang et al, 2008; Park et al., 2008a). In these studies we also discovered that in addition to well recognized components of the CD95-DISC, e.g. pro-caspase 8, c-FLIP-s, we also observed increased association of autophagy and ER stress regulatory proteins, e.g. ATG5, Grp78/BiP. Hence, we examined the roles of CD95 and c-FLIP-s in modulating sorafenib+vorinostat toxicity in both HCT116 and in SW480 cells. Knock down of CD95 *increased* vorinostat and sorafenib+vorinostat toxicity in HCT116 cells, and over-expression of c-FLIP-s weakly blunted drug –induced cell killing (Figure 1C). Knock down of CD95 or over-expression of c-FLIP-s blocked sorafenib+vorinostat toxicity in SW480 cells (Figure 1D). The data obtained in SW480 cells is very similar to that previously noted in liver, pancreatic and kidney cancer cells. In

Molecular Pharmacology Fast Forward. Published on May 29, 2009 as DOI: 10.1124/mol.109.056523
This article has not been copyedited and formatted. The final version may differ from this version.

HCT116 cells, sorafenib+vorinostat exposure caused the association of pro-caspase 8 and the chaperone Grp78/BiP with CD95 but did not increase plasma membrane staining for CD95 (Figure 1E). In HCT116 cells the amount of c-FLIP-s associated with pro-caspase 8 in the DISC was weakly increased after drug exposure. In SW480 cells, but not matched SW620 cells, sorafenib+vorinostat exposure profoundly increased CD95 plasma membrane staining; drug treatment in SW480 cells caused the association of pro-caspase 8 and Grp78/BiP with CD95 and with reduced expression of c-FLIP-s in the DISC (Figure 1F) (Kubens et al, 1998).

Over-expression of BCL-XL or expression of dominant negative caspase 9 suppressed sorafenib+vorinostat toxicity in HCT116 cells, arguing that in this cell line the drugs were using the intrinsic pathway to kill (Figure 2A). As mitochondrial dysfunction was playing a role in sorafenib+vorinostat lethality in HCT116 cells, we then determined whether inhibition of protective BCL-2 family members facilitated drug-induced cell killing. Treatment of cells with pharmacologically achievable concentrations of the BCL-2 / BCL-XL / MCL-1 inhibitor GX15-070 (Obatoclax) significantly increased HCT116 or SW480 cell mortality (Figures 2B and 2C) (Nguyen et al, 2007). GX15-070 as a single agent was more toxic in HCT116 cells than in SW480 cells, and in HCT116 cells GX15-070 did not strongly enhance the toxicity of sorafenib+valproate exposure. In SW480 cells, however, GX15-070 increased short-term sorafenib+valproate lethality in at least an additive fashion. A similar effect was observed in SW480 cells using long-term colony formation assays (data not shown). Of particular note, the toxic interaction in HCT116 cells between sorafenib and the class I HDACI sodium valproate was greater than the interaction between sorafenib and the pan-HDACI vorinostat. Valproic acid has been shown to affect HDAC2 levels by inducing its proteasomal degradation, although whether altered HDAC2 function represents the reason for this observation will require future study (Kramer et al, 2003).

Loss of CD95 expression is common in tumors from patients with metastatic / advanced colon cancer, and as such, we next determined whether GX15-070 could facilitate sorafenib+valproate lethality in SW480 cells with reduced CD95 function. Knock down of CD95 significantly reduced sorafenib+valproate –induced killing in SW480 cells (Figure 2D). In CD95 knock down cells treated with GX15-070, however, no significant reduction

Molecular Pharmacology Fast Forward. Published on May 29, 2009 as DOI: 10.1124/mol.109.056523
This article has not been copyedited and formatted. The final version may differ from this version.

in sorafenib + valproate + GX15-070 lethality was observed, compared to scrambled siRNA control transfected cells. We then determined whether GX15-070 also enhanced the toxicity of sorafenib + HDACI treatment in other tumor cell types. GX15-070 increased sorafenib+valproate lethality in at least an additive fashion in short-term assays in adult human ovarian cancer cells and in human pediatric rhabdomyosarcoma cells (Figures 2E and 2F). As was observed in HCT116 cells, sodium valproate enhanced sorafenib toxicity in these cell types to a greater extent than did vorinostat. Knock down of CD95 suppressed sorafenib + HDACI toxicity in ovarian cancer and in rhabdomyosarcoma cells, an effect that was circumvented by GX15-070 (Figures 2G and 2H). Sorafenib + HDACIs synergized to kill rhabdomyosarcoma cells in colony formation assays (Table 3). Collectively the data in Figure 2 demonstrate in multiple types of tumor cell that sorafenib + HDACI lethality is enhanced by an agent which inhibits protective BCL-2 protein function.

In our prior studies using hepatoma cells, we had noted that CD95 activation was inhibited by small molecule inhibitors of the de novo ceramide synthesis pathway, as well as by knock down or knock out of acidic sphingomyelinase (ASMase). As noted previously, compared to patient matched SW480 cells, SW620 cells were refractory to drug-induced toxicity that correlated with a lack of CD95 activation (Figure 1D). It has recently been shown that SW620 cells are refractory to death receptor signaling induced by tumor necrosis factor-related apoptosis-inducing ligand (TRAIL) which was linked to low expression of ceramide synthase 6 (LASS6), an enzyme in the de novo ceramide synthesis pathway, and with a lack of ceramide generation after TRAIL exposure (White-Gilbertson et al., 2009). Knock down of ASMase expression or treatment with the de novo pathway inhibitor myriocin blocked sorafenib + vorinostat –induced CD95 activation in SW480 cells (Figure 3A). Knock down of LASS6 expression in SW480 cells also reduced drug-induced CD95 activation and drug-induced cell killing (Figure 3B, data not shown). Similar data with respect to reduced CD95 activation when LASS 6 was knocked down were also observed in liver, pancreatic and ovarian cells (Figure 3B). Knock down of ASMase expression or treatment with the de novo pathway inhibitor myriocin blocked sorafenib + vorinostat –induced cell killing in SW480 cells (Figure 3C). Based on the data in Figure 3A, we determined whether expression of LASS6 in SW620 cells facilitated drug-induced CD95 activation and cell death. Over-

Molecular Pharmacology Fast Forward. Published on May 29, 2009 as DOI: 10.1124/mol.109.056523
This article has not been copyedited and formatted. The final version may differ from this version.

expression of LASS6 in SW620 cells enhanced the toxicity of sorafenib, vorinostat and the drug combination which correlated with increased activation of CD95 (Figure 3D). Collectively, this data argues that expression of enzymes within the de novo ceramide pathway, particularly LASS6, is essential for CD95 activation and for the toxic actions of sorafenib and vorinostat in SW480 / SW620 colon cancer cells.

We next performed studies to understand how knock down of CD95 *enhanced* sorafenib + vorinostat toxicity in HCT116 cells. In hepatoma cells we have previously noted that sorafenib+vorinostat exposure promoted a protective form of autophagy in a CD95- and PERK- / eIF2α- dependent fashion. In HCT116 colon cancer cells sorafenib+vorinostat exposure promoted increased phosphorylation of PERK and the processing of LC3 (ATG8) which are suggestive of increased levels of autophagy (Figure 4A). Grp78/BiP is a chaperone for PERK and dissociates from PERK permitting PERK to be activated, and of note, we previously demonstrated that Grp78/BiP became associated with CD95 after drug exposure (Figure 1C) (Park et al., 2008a). However, despite PERK becoming phosphorylated after drug treatment, no increase in the phosphorylation of the PERK substrate eIF2α was observed. In HCT116 cells sorafenib+vorinostat exposure promoted vesicularization of a transfected LC3-GFP construct, also indicative of increased autophagy, an effect which was blocked by expression of dominant negative PERK, and by knock down of either ATG5 or Beclin1 (Figures 4B and 4C). Expression of dominant negative PERK blocked drug-induced increases in PERK phosphorylation, the processing of LC3, and drug-induced activation of the JNK pathway (Figure 4B). Knock down of CD95 expression in HCT116 cells abolished drug-induced autophagy (Figure 4C). We then determined whether drug-induced autophagy was a protective or a toxic signal; knock down of Beclin1 expression enhanced both vorinostat and sorafenib+vorinostat lethality (Figure 4D). In general agreement with prior findings in liver, pancreatic and kidney cancer cells, knock down of Beclin1 in SW480 cells also abolished drug-induced autophagy and enhanced sorafenib + vorinostat toxicity (data not shown). Collectively, the data in Figure 4, together with those presented in Figure 1, demonstrate that sorafenib+vorinostat treatment promote a form of

CD95 activation in HCT116 cells that is non-productive with respect to pro-apoptotic signaling but is competent to stimulate an autophagic response that is cyto-protective.

We next determined whether drug-induced PERK signaling through the JNK pathway was regulated by CD95 and whether JNK pathway signaling also played a role in the regulation of autophagy. Sorafenib + vorinostat treatment activated the JNK pathway but not the p38 MAPK pathway (Figure 5A, upper blots). Inhibition of the JNK pathway enhanced the toxicity of sorafenib + vorinostat treatment (Figure 5A, lower graph). Knock down of CD95 expression blocked JNK pathway activation however, unlike prior data in hepatoma cells knock down of CD95 did not alter PERK activation (Figure 5B, upper blots). Thus JNK1/2 activation requires separate drug-induced signals emanating from both CD95 and PERK.

We then examined whether JNK pathway signaling played any regulatory role in autophagy induction. Molecular inhibition of JNK1/2 signaling blocked drug-induced vesicularization of LC3-GFP (Figure 5B, lower graph). The autophagy regulatory protein Beclin1 has been shown to bind to BCL-2, and phosphorylation of BCL-2 by JNK1 has been proposed to cause Beclin1 to dissociate from BCL-2, thereby promoting a protective form of autophagy (Wei et al, 2008). In HCT116 cells Beclin1 co-immunoprecipitated with BCL-2 and co-precipitation of the Beclin1 with BCL-2 was almost abolished in cells treated with sorafenib and sodium valproate (Figure 5C). The association of Beclin1 with BCL-2 was maintained by inhibition of JNK pathway signaling, that correlated with inhibition of autophagy (Figures 5B and 5C).

Sorafenib was developed as an inhibitor of Raf kinases, however is now known to inhibit class III receptor tyrosine kinases. In HCT116 cells sorafenib+vorinostat exposure did not alter AKT (S473) phosphorylation (Figure 6A). In a similar manner to findings in hepatoma cells, sorafenib+vorinostat exposure transiently inhibited ERK1/2 activity, 48h after exposure. Based on this data, we used molecular approaches to define the role of each pathway in the survival response of drug treated HCT116 cells. Transient expression of dominant negative MEK1, but not dominant negative AKT, enhanced the toxicity of sorafenib, vorinostat and the drug

combination (Figure 6A). In general agreement with our data in Figure 6A transient expression of activated MEK1 EE but not expression of activated AKT, suppressed sorafenib+vorinostat toxicity in HCT116 cells (Figure 6B). Thus the ERK1/2 pathway plays a greater regulatory role than the AKT pathway in HCT116 cells.

Molecular Pharmacology Fast Forward. Published on May 29, 2009 as DOI: 10.1124/mol.109.056523
This article has not been copyedited and formatted. The final version may differ from this version.

Discussion

The present studies were designed to examine whether sorafenib and HDACIs interact in a synergistic manner to cause cell death in colon cancer cells. In short term cell viability assays, sorafenib and vorinostat caused an additive to greater than additive increase in colon cancer cell death. In cells where short-term lethality for the combination was greater than additive, a strong activation of CD95 was observed. In long-term colony formation assays, regardless of short-term CD95 activation, sorafenib and vorinostat treatment synergized to kill colon cancer cells with CI values of less than 0.70. Collectively, our findings in colon cancer cells with respect to the toxicity of sorafenib and HDACI treatment are in general agreement with those in NSCLC, renal, liver, melanoma and pancreatic cancer cells (Zhang et al, 2008; Park et al, 2008).

In agreement the concept that reduced basal activity in the MEK1/2 and/or PI3K pathways will reduce cellular tumorigenicity and diminish the toxicity of drugs targeting protein and lipid kinases, we found that the lethality of sorafenib or vorinostat, or the drug combination was suppressed by deletion of K-RAS D13 from HCT116 cells. This is of note because HCT116 cells lacking K-RAS D13 expression are considered only semi-transformed and do not form colonies in soft agar or tumors in animals. We then investigated the relative importance of three of the best defined pathways downstream of RAS proteins that were likely to be involved in controlling drug toxicity: Raf-MEK1/2 (H-RAS V12 S35); PI3K-AKT (H-RAS V12 C40); RAL GDS (H-RAS V12 G37). We have recently published using these cells in vitro and in vivo that activation of RAS predicted resistance to PI3K inhibitors even in the presence of activating PI3K mutations or loss of PTEN, whereas H-RAS V12 (C40) –induced single activation of PI3K predicted for sensitivity to PI3K inhibitors (Ihle et al., 2009). Expression of H-RAS V12 but not point effector mutants of H-RAS V12 that activate PI3K-AKT (C40) or RAL GDS (G37) restored the toxicity of sorafenib or vorinostat, and the drug combination, to near those levels observed in wild type cells. In contrast to data with other effector point mutants, expression of the mutant H-RAS that elevates Raf-MEK1/2 signaling enhanced both vorinostat and sorafenib+vorinostat lethality above those in parental cells or cells expressing wild type H-RAS V12. However, we also found in wild type HCT116 cells that *transient* expression of dominant negative MEK1 enhanced the toxicity of sorafenib, vorinostat and

Molecular Pharmacology Fast Forward. Published on May 29, 2009 as DOI: 10.1124/mol.109.056523
This article has not been copyedited and formatted. The final version may differ from this version.

sorafenib+vorinostat. *Transient* expression of activated MEK1 also suppressed the toxicity of sorafenib, vorinostat and sorafenib+vorinostat. It is known that HDACI lethality can be enhanced when ERK1/2 pathway signaling is inhibited using potent small molecule MEK1/2 inhibitors (Yu et al, 2005; Ozaki et al, 2006). Sorafenib toxicity can also be enhanced by small molecule MEK1/2 inhibitors (S. Grant, unpublished observation). Collectively, our data in HCT116 cells leads us to conclude that whilst transient inhibition of ERK1/2 signaling can promote the toxicity vorinostat and facilitate sorafenib+vorinostat killing, sustained elevated basal levels of ERK1/2 activity within colon cancer cells are also predictive for enhanced vorinostat toxicity as well as enhanced sorafenib+vorinostat toxicity.

In our prior studies combining sorafenib and vorinostat in NSCLC, renal, liver, melanoma and pancreatic cancer cells, cell killing was PERK- and CD95 dependent and the induction of protective autophagy was also PERK- and CD95 dependent. We noted in SW480, OVCAR, and Rh41 cells that a similar mechanism of drug action via CD95 also was extant. In HCT116 cells, however, although PERK was activated in a CD95 dependent fashion, eIF2α phosphorylation did not increase. Drug-induced eIF2α phosphorylation was previously noted to be essential for translational repression of c-FLIP-s and MCL-1 levels and in HCT116 cells, the levels of neither c-FLIP-s nor MCL-1 were suppressed after drug treatment, and the levels of c-FLIP-s remained elevated in the CD95 DISC (Park et al, 2008a). This data may explain why CD95-caspase 8 signaling was non-productive in HCT116 cells. To our surprise we found that knock down of CD95 expression in HCT116 cells increased cell killing. However, we noted that drug exposure promoted a protective form of autophagy that was CD95 dependent. This data confirms and extends our prior work and argues that in some cell types and under certain treatment conditions, death receptor signaling promotes cell survival through increased autophagy.

It has been widely reported that the expression / function of CD95 can be reduced or lost in metastatic colon cancer. We determined that a clinically relevant small molecule antagonist of BCL-2 family proteins that is entering phase II trials (GX15-070; Obatoclax) enhanced sorafenib+HDACI lethality, and in cells where knock down of CD95 reduced sorafenib+HDACI toxicity, Obatoclax was capable of reverting sorafenib+HDACI

Molecular Pharmacology Fast Forward. Published on May 29, 2009 as DOI: 10.1124/mol.109.056523
This article has not been copyedited and formatted. The final version may differ from this version.

lethality to levels approaching those in vector control transfected cells; this finding was relevant in multiple tumor cell types. Additional studies will be required to determine which BH3 domain only proteins play a central role in the death-promoting biologic effects of Obatoclax in colon cancer cells.

We have shown that bile acids can promote ligand independent, acidic sphingomyelinase (ASMase) and ceramide –dependent, activation of CD95 in primary hepatocytes and that generated both toxic signals (caspase 8 and JNK1 activation) as well as protective signals (JNK2 activation) (Qiao et al, 2002; Qiao et al, 2003). The generation of ceramide has been shown by many groups to promote ligand independent activation of several growth factor receptors via the localization / clustering of these receptors and other signal facilitating proteins into lipid rich domains (Barnhart et al, 2003; Kolesnick and Fuks, 2003). In melanoma, renal and liver cancer cells, combined but not individual exposure to sorafenib and vorinostat, caused rapid activation of CD95 that did not correlate with altered expression or cleavage of FAS-L (Zhang et al, 2008).

In SW480 cells, sorafenib and vorinostat exposure activated CD95 as judged by increased plasma membrane staining for CD95 as well as increased DISC formation in an ASMase- and de novo –ceramide synthesis pathway dependent fashion. However, in patient matched SW620 cells that have reduced ceramide synthase 6 (LASS6) expression activation of CD95 was not observed. Our prior analyses in sorafenib+vorinostat treated HEPG2 cells demonstrated that inhibition of the de novo synthesis pathway suppressed generation of multiple dihydro-ceramide species, particularly the C12 / C14 / C16 dihydro-ceramides. The six known ceramide synthase genes (LASS) are localized in the ER and different LASS proteins have been noted to generate different chain length ceramide forms, with LASS5 and LASS6 being most closely linked to the generation of C14 and C16 dihydro ceramide (Ogretmen and Hannun, 2004; Futerman and Riezman, 2005). In general agreement with the hypothesis that LASS6 is a key player in the regulation of sorafenib and vorinostat toxicity, knock down of LASS6 in SW480 cells suppressed drug-induced CD95 activation and cell killing whereas expression of LASS6 in SW620 cells enhanced drug-induced CD95 activation and cell killing. Similar findings were also made in ovarian, liver and pancreatic tumor cells. Whether the expression and / or the activities of

Molecular Pharmacology Fast Forward. Published on May 29, 2009 as DOI: 10.1124/mol.109.056523
This article has not been copyedited and formatted. The final version may differ from this version.

LASS proteins are regulated by a combination of vorinostat-modulated protein acetylation and sorafenib-induced changes in ROS and Ca^{2+} fluxes in the ER will need to be carefully examined in future studies.

In some cell types, the toxicity of vorinostat has been linked to activation of the JNK pathway (Yu et al, 2003; Portanova et al, 2008). In HCT116 cells we noted that vorinostat and sorafenib+vorinostat exposure increased the phosphorylation of JNK1/2, indicative of kinase activation. However, in hepatoma and renal carcinoma cells, or in SW480 cells, at the drug concentrations used in this study, the activations of JNK1/2 were either modest or not observed (Park, Walker and Dent, Unpublished observations). Signaling by the JNK pathway has been linked to growth promoting signals as well as both pro- and anti-apoptotic regulation (Qiao et al, 2003; Wang et al, 2006; Liu et al, 2004; Hochedlinger et al, 2002). Inhibition of JNK1/2 using a molecular tool modestly *enhanced* sorafenib+vorinostat toxicity in HCT116 cells; our somewhat surprising finding became more easily understood when we noted that activation of JNK1/2 was dependent on expression of CD95 and was blocked by expression of dominant negative PERK. JNK signaling decreased the amount of Beclin1 co-precipitating with BCL-2 and in drug-treated cells lacking JNK activation more Beclin1 remained associated with BCL-2 than under vehicle or drug treatment conditions in the absence of JNK pathway blockade. This is in agreement with the concept that JNK signaling regulates the Beclin1-BCL-2 interaction, wherein JNK signaling promotes autophagy by causing Beclin1 release from BCL-2 (Wei et al, 2008). Further analysis of the upstream molecular events that regulate JNK pathway activation by CD95 and PERK will require studies beyond the scope of the present manuscript.

In conclusion, sorafenib and vorinostat interact to kill multiple colon cancer cell types. Unlike tumor cell types previously examined, such as NSCLC, renal, liver, melanoma and pancreatic cancer cells, cell killing in colon cancer cells occurs via both CD95-dependent and CD95-independent mechanisms. Though in all tumor cell types examined thus far, the induction of mitochondrial dysfunction and activation of the intrinsic pathway play central roles in drug lethality. Further studies will be required to translate the findings of this manuscript for colon cancer into animal models and ultimately the clinic.

References.

Allan LA, Morrice N, Brady S, Magee G, Pathak S, Clarke PR. (2003) Inhibition of caspase-9 through phosphorylation at Thr 125 by ERK MAPK. Nat Cell Biol **5**:647–54.

Bali P, Pranpat M, Swaby R, et al. (2005) Activity of suberoylanilide hydroxamic Acid against human breast cancer cells with amplification of her-2. Clin Cancer Res **11**: 6382-9.

Barnhart BC, Alappat EC, Peter ME. (2003) The CD95 type I/type II model. Semin Immunol **15**:185-93.

Dasmahapatra G, Yerram N, Dai Y, Dent P, Grant S. (2007) Synergistic interactions between vorinostat and sorafenib in chronic myelogenous leukemia cells involve Mcl-1 and p21CIP1 down-regulation. Clin Cancer Res **13**:4280-90.

Davies BR, Logie A, McKay JS, et al. (2007) AZD6244 (ARRY-142886), a potent inhibitor of mitogen-activated protein kinase/extracellular signal-regulated kinase kinase 1/2 kinases: mechanism of action in vivo, pharmacokinetic/pharmacodynamic relationship, and potential for combination in preclinical models. Mol Cancer Ther **6**:2209-19.

Dent, P. (2005) MAP kinase pathways in the control of hepatocyte growth, metabolism and survival. Signaling Pathways in Liver Diseases, Springer Press. Chapter 19. pp 223-238 Eds. J.F. Dufour P.-A. Clavien.

Dent P, Yacoub A, Fisher PB, Hagan MP, Grant S. (2003) MAPK pathways in radiation responses. Oncogene **22**:5885-96.

Flaherty KT. (2007) Sorafenib: delivering a targeted drug to the right targets. Expert Rev Anticancer Ther **7**:617-26.

Futerman, A. H.; Riezman, H. (2005) The ins and outs of sphingolipid synthesis. Trends Cell Biol. **15**:312–318.

Gollob JA. (2005) Sorafenib: scientific rationales for single-agent and combination therapy in clear-cell renal cell carcinoma. Clin Genitourin Cancer **4**:167-74.

Grant S, Dent P. (2004) Kinase inhibitors and cytotoxic drug resistance. Clin Cancer Res **10**:2205-7.

Gregory P. D., Wagner K., Horz W. (2001) Histone acetylation and chromatin remodeling. Exp. Cell Res **265**: 195-202.

Hegde SR, Sun W, Lynch JP. (2008) Systemic and targeted therapy for advanced colon cancer. Expert Rev Gastroenterol Hepatol. **2**:135-49.

Hochedlinger K, Wagner EF, Sabapathy K. (2002) Differential effects of JNK1 and JNK2 on signal specific induction of apoptosis. Oncogene. **21**:2441-5

Ihle N, Lemos R, Wipf P, Yacoub A, Mitchell C, Siwak D, Mills G, Dent P, Lirkpatrick L, Powis, G. (2009) Activating PI-3-kinase mutation confers sensitivity, while oncogenic Ras mutation confers resistance to PI-3-kinase inhibition. Cancer Res. **69**: 143-50.

Kolesnick R., Fuks Z. (2003) Radiation and ceramide-induced apoptosis. Oncogene. **22**:5897–5906.

Krämer OH, Zhu P, Ostendorff HP, Golebiewski M, Tiefenbach J, Peters MA, Brill B, Groner B, Bach I, Heinzel T, Göttlicher M. (2003) The histone deacetylase inhibitor valproic acid selectively induces proteasomal degradation of HDAC2. EMBO J. **22**: 3411-20.

Kubens BS, Zänker KS. (1998) Differences in the migration capacity of primary human colon carcinoma cells (SW480) and their lymph node metastatic derivatives (SW620). Cancer Lett. **131**:55-64.

Kwon SH, Ahn SH, Kim YK, et al. (2002) Apicidin, a histone deacetylase inhibitor, induces apoptosis and Fas/Fas ligand expression in human acute promyelocytic leukemia cells. J Biol Chem **277**: 2073-80.

Ley R, Balmanno K, Hadfield K, Weston C, Cook SJ. (2003) Activation of the ERK1/2 signaling pathway promotes phosphorylation and proteasome-dependent degradation of the BH3-only protein, Bim. J Biol Chem **278**:18811–6.

Li N, Batt D, Warmuth M. (2007) B-Raf kinase inhibitors for cancer treatment. Curr Opin Investig Drugs **8**:452-6.

Liu J, Minemoto Y, Lin A. (2004) c-Jun N-terminal protein kinase 1 (JNK1), but not JNK2, is essential for tumor necrosis factor alpha-induced c-Jun kinase activation and apoptosis. Mol Cell Biol. **24**:10844-56.

Marks PA, Miller T, and Richon VM. (2003) Histone deacetylases. Curr Opin Pharmacol **3**: 344-351.

Martin AP, Miller A, Emad L, Rahmani M, Walker T, Mitchell C, Hagan MP, Park MA, Yacoub A, Fisher PB, Grant S, Dent P. (2008) Lapatinib resistance in HCT116 cells is mediated by elevated MCL-1 expression and decreased BAK activation and not by ERBB receptor kinase mutation. Mol Pharmacol. **74**:807-22.

Mitchell C, Park MA, Zhang G, Han SI, Harada H, Franklin RA, Yacoub A, Li PL, Hylemon PB, Grant S, Dent P. (2007) 17-Allylamino-17-demethoxygeldanamycin enhances the lethality of deoxycholic acid in primary rodent hepatocytes and established cell lines. Mol Cancer Ther **6**: 618-32.

Mori M, Uchida M, Watanabe T, et al. (2003) Activation of extracellular signal-regulated kinases ERK1 and ERK2 induces Bcl-xL up-regulation via inhibition of caspase activities in erythropoietin signaling. J Cell Physiol **195**:290–7.

Nguyen M, Marcellus RC, Roulston A, Watson M, Serfass L, Murthy Madiraju SR, Goulet D, Viallet J, Bélec L, Billot X, Acoca S, Purisima E, Wiegmans A, Cluse L, Johnstone RW, Beauparlant P, Shore GC. (2007) Small molecule obatoclax (GX15-070) antagonizes MCL-1 and overcomes MCL-1-mediated resistance to apoptosis. Proc Natl Acad Sci U S A. **104**: 19512-7.

Ogretmen B., Hannun Y. A. (2004) Biologically active sphingolipids in cancer pathogenesis and treatment. Nat. Rev. Cancer. **4**:604–616.

Ozaki K, Minoda A, Kishikawa F, Kohno M. (2006) Blockade of the ERK pathway markedly sensitizes tumor cells to HDAC inhibitor-induced cell death. Biochem Biophys Res Commun. **339**: 1171-7.

Pang RW, Poon RT. (2007) From molecular biology to targeted therapies for hepatocellular carcinoma: the future is now. Oncology **72** Suppl 1: 30-44.

Park MA, Zhang G, Martin AP, Hamed H, Mitchell C, Hylemon PB, Graf M, Rahmani M, Ryan K, Liu X, Spiegel S, Norris J, Fisher PB, Roberts JD, Grant S, Dent P. (2008a) Vorinostat and sorafenib increase ER stress, autophagy and apoptosis via ceramide-dependent CD95 and PERK activation. Cancer Biol & Ther **7**: 135-149.

Park MA, Yacoub A, Rahmani M, et al. (2008b) OSU-03012 stimulates PERK-dependent increases in HSP70 expression, attenuating its lethal actions in transformed cells. Mol Pharm. **73**: 1168-84.

Park MA, Zhang G, Mitchell C, Rahmani M, Hamed H, Hagan MP, Yacoub A, Curiel DT, Fisher PB, Grant S and Dent P. (2008c) Mitogen-activated protein kinase kinase 1/2 inhibitors and 17-allylamino-17-demethoxygeldanamycin synergize to kill human gastrointestinal tumor cells *in vitro* via suppression of c-FLIP-s levels and activation of CD95. Mol Cancer Ther **7**: 2633-2648.

Parkin DM, Bray F, Ferlay J, Pisani P. (2005) Global cancer statistics, 2002. CA Cancer J Clin **55**:74–108.

Portanova P, Russo T, Pellerito O, Calvaruso G, Giuliano M, Vento R, Tesoriere G. (2008) The role of oxidative stress in apoptosis induced by the histone deacetylase inhibitor suberoylanilide hydroxamic acid in human colon adenocarcinoma HT-29 cells. Int J Oncol. **33**:325-31.

Qiao L, Studer E, Leach K, et al. (2001) Deoxycholic acid (DCA) causes ligand-independent activation of epidermal growth factor receptor (EGFR) and FAS receptor in primary hepatocytes: inhibition of EGFR/mitogen-activated protein kinase-signaling module enhances DCA-induced apoptosis. Mol Biol Cell **12**:2629-45.

Qiao L, Han SI, Fang Y, Park JS, Gupta S, Gilfor D, Amorino G, Valerie K, Sealy L, Engelhardt JF, Grant S, Hylemon PB, Dent P. (2003) Bile acid regulation of C/EBPbeta, CREB, and c-Jun function, via the extracellular signal-regulated kinase and c-Jun NH2-terminal kinase pathways, modulates the apoptotic response of hepatocytes. Mol Cell Biol. **23**:3052-66.

Qiao L, Yacoub A, Studer E, Gupta S, Pei XY, Grant S, Hylemon PB, Dent P. (2002) Inhibition of the MAPK and PI3K pathways enhances UDCA-induced apoptosis in primary rodent hepatocytes. Hepatology. **35**:779-89.

Rahmani M, Davis EM, Bauer C, Dent P, Grant S. (2005) Apoptosis induced by the kinase inhibitor BAY 43-9006 in human leukemia cells involves down-regulation of Mcl-1 through inhibition of translation. J Biol Chem **280**:35217-27.

Rahmani M, Nguyen TK, Dent P, Grant S. (2007a) The multikinase inhibitor sorafenib induces apoptosis in highly imatinib mesylate-resistant bcr/abl+ human leukemia cells in association with signal transducer and activator of transcription 5 inhibition and myeloid cell leukemia-1 down-regulation. Mol Pharmacol **72**:788-95.

Rahmani M, Davis EM, Crabtree TR, et al. (2007b) The kinase inhibitor sorafenib induces cell death through a process involving induction of endoplasmic reticulum stress. Mol Cell Biol. **27**:5499-513.

Rini BI. (2006) Sorafenib. Expert Opin Pharmacother. **7**:453-61.

Strumberg D. (2005) Preclinical and clinical development of the oral multikinase inhibitor sorafenib in cancer treatment. Drugs Today (Barc) **41**:773-84.

Valerie K, Yacoub A, Hagan MP, et al. (2007) Radiation-induced cell signaling: inside-out and outside-in. Mol Cancer Ther **6**:789-801.

Venturelli S, Armeanu S, Pathil A, et al. (2007) Epigenetic combination therapy as a tumor-selective treatment approach for hepatocellular carcinoma. Cancer. **109**: 2132-41.

Wang YF, Jiang CC, Kiejda KA, Gillespie S, Zhang XD, Hersey P. (2007) Apoptosis induction in human melanoma cells by inhibition of MEK is caspase-independent and mediated by the Bcl-2 family members PUMA, Bim, and Mcl-1. Clin Cancer Res **13**:4934-42.

Wang Y, Singh R, Lefkowitch JH, Rigoli RM, Czaja MJ. (2006) Tumor necrosis factor-induced toxic liver injury results from JNK2-dependent activation of caspase-8 and the mitochondrial death pathway. J Biol Chem. **281**:15258-67.

Wei Y, Pattingre S, Sinha S, Bassik M, Levine B. (2008) JNK1-mediated phosphorylation of Bcl-2 regulates starvation-induced autophagy. Mol Cell. **30**: 678-88.

White-Gilbertson S, Mullen T, Senkal C, Lu P, Ogretmen B, Obeid L, Voelkel-Johnson C. (2009) Ceramide synthase 6 modulates TRAIL sensitivity and nuclear translocation of active caspase-3 in colon cancer cells.Oncogene. **28**:1132-41.

Wise LD, Turner KJ, Kerr JS. (2007) Assessment of developmental toxicity of vorinostat, a histone deacetylase inhibitor, in Sprague-Dawley rats and Dutch Belted rabbits. Birth Defects Res B Dev Reprod Toxicol **80**: 57-68.

Yacoub A, Park MA, Gupta P, et al. (2008) Caspase-, cathepsin- and PERK-dependent regulation of MDA-7/IL-24-induced cell killing in primary human glioma cells. Mol Cancer Ther **7**: 297-313.

Yu C, Subler M, Rahmani M, Reese E, Krystal G, Conrad D, Dent P, Grant S. (2003) Induction of apoptosis in BCR/ABL+ cells by histone deacetylase inhibitors involves reciprocal effects on the RAF/MEK/ERK and JNK pathways. Cancer Biol Ther. **2**:544-51.

Yu C, Dasmahapatra G, Dent P, Grant S. (2005) Synergistic interactions between MEK1/2 and histone deacetylase inhibitors in BCR/ABL+ human leukemia cells. Leukemia. **19**:1579-89.

Zhang G, Park M, Mitchell C, et al. (2008) Vorinostat and sorafenib synergistically kill tumor cells via FLIP suppression and CD95 activation. Clin Cancer Res **14**: 5385-99.

Molecular Pharmacology Fast Forward. Published on May 29, 2009 as DOI: 10.1124/mol.109.056523
This article has not been copyedited and formatted. The final version may differ from this version.

Footnotes.

This work was funded; to P.D. from Public Health Service grants [R01-DK52825, P01-CA104177, R01-CA108520, R01-CA63753; R01-CA77141]. These studies were also funded in part by The Jimmy V Foundation and by The Godwin Foundation. PD is the holder of the Universal Inc. Professorship in Signal Transduction Research.

Molecular Pharmacology Fast Forward. Published on May 29, 2009 as DOI: 10.1124/mol.109.056523
This article has not been copyedited and formatted. The final version may differ from this version.

Figure Legends

Figure 1. Sorafenib and vorinostat interact to kill multiple human colon cancer cell lines. Panel A. SW620, SW480, DLD-1 and HCT116 cells were treated with vehicle, sorafenib, vorinostat or sorafenib + vorinostat. Ninety six hours after exposure, cells were isolated and viability determined via trypan blue exclusion assay (± SEM, n = 3 independent studies) * $p < 0.05$ lower than corresponding value in SW480 cells. **Panel B.** Parental and transfected variants of HCT116 cells were treated with vehicle, sorafenib, vorinostat or sorafenib + vorinostat. Forty eight hours after exposure, cells were isolated and stained with Annexin V – propidium iodide and cell viability determined by flow cytometry (± SEM, n = 3) # $p < 0.05$ greater than sorafenib or vorinostat treatment alone; ## $p < 0.05$ greater than corresponding value in parental + CMV vector cells; * $p < 0.05$ less than corresponding value in parental + CMV vector cells; ** $p < 0.05$ less than corresponding value in K-RAS D13 null + H-RAS V12 cells. Inset panel: immunoblotting of untreated cells for the basal levels of phosphorylation of ERK1/2 and AKT (S473; T308) in the HCT116 isolates. **Panel C. and Panel D.** HCT116 or SW480 cells were, as indicated, either infected with recombinant adenoviruses, or were transfected with siRNA molecules to knock down CD95. Twenty four h after infection or transfection, cells were treated with vehicle, sorafenib, vorinostat or both drugs together. Forty eight hours after exposure, cells were isolated and stained with Annexin V – propidium iodide and cell viability determined by flow cytometry (± SEM, n = 3) * $p < 0.05$ less than corresponding value in CMV vector or siSCR control cells. Immunoblotting panels show CD95 knock down and c-FLIP-s protein expression under the indicated conditions. **Panel E. and Panel F.** HCT116, SW480 and SW620 cells were plated in 8 well glass chamber slides and were treated with vehicle or sorafenib + vorinostat. Cells were fixed and not permeabilized 0-8h after drug exposure. Fixed cells were immuno-stained for plasma membrane associated CD95 and visualized using an FITC conjugated secondary antibody. Images are representatives from two separate studies. In parallel HCT116 and SW480 cells were treated with vehicle or with sorafenib + vorinostat. Six h after treatment cells were lysed and CD95 immunoprecipitated. Immunoprecipitates were subjected to SDS PAGE and immunoblotting. A representative CD95 immunoprecipitate is shown (n = 3).

Molecular Pharmacology Fast Forward. Published on May 29, 2009 as DOI: 10.1124/mol.109.056523
This article has not been copyedited and formatted. The final version may differ from this version.

Figure 2. Sorafenib and vorinostat toxicity is enhanced by GX15-070 in SW480 cells. Panel A. HCT116 cells were, as indicated, infected with recombinant adenoviruses and 24h after infection, cells were treated with vehicle, sorafenib, vorinostat or both drugs together. Forty eight hours after exposure, cells were isolated and stained with Annexin V – propidium iodide and cell viability determined by flow cytometry (± SEM, n = 3) * $p < 0.05$ less than corresponding value in CMV vector cells. Inset Panel: expression of BCL-XL 24h after infection. **Panel B.** HCT116 cells were treated with vehicle or GX15-070 followed by, as indicated, vehicle, sorafenib, sodium valproate or sorafenib + valproate. Twenty four h and 48h after exposure, cells were isolated and viability determined via Annexin V – propidium iodide and cell viability determined by flow cytometry (± SEM, n = 3 independent studies). # $p < 0.05$ greater than corresponding value in HCT116 cells (*cf Figure 1, Panel B*). **Panel C.** SW480 cells 24h after plating in triplicate, were treated with vehicle or GX15-070 followed by, as indicated, vehicle (DMSO), sorafenib, sodium valproate or sorafenib + valproate. Twenty four h and 48h after exposure, cells were isolated and viability determined via Annexin V – propidium iodide and cell viability determined by flow cytometry (± SEM, n = 3 independent studies). **Panel D.** SW480 cells were transfected with siRNA molecules to knock down CD95. Twenty four h after transfection cells were treated with vehicle or GX15-070 followed by, as indicated, vehicle, sorafenib, sodium valproate or sorafenib + valproate. Twenty four h and 48h after exposure, cells were isolated and viability determined via Annexin V – propidium iodide and cell viability determined by flow cytometry (± SEM, n = 2 independent studies). * $p < 0.05$ less than corresponding value in siSCR transfected cells. **Panels E.** and **F.** OVCAR and SKOVIII, and Rh30 and Rh41, cells were treated with vehicle or GX15-070 followed by, as indicated, vehicle, sorafenib, vorinostat, sodium valproate or sorafenib + valproate or sorafenib+vorinostat. Forty eight h after exposure, cells were isolated and viability determined via trypan blue exclusion assay (± SEM, n = 3 independent studies). # $p < 0.05$ greater than sorafenib + vorinostat value. **Panels G** and **H.** OVCAR and Rh41 cells were transfected with siRNA molecules to knock down CD95. Twenty four h after transfection cells were treated with vehicle or GX15-070 followed by, as indicated, vehicle, sorafenib, sodium valproate or sorafenib + valproate. Twenty four h and 48h after exposure, cells were isolated and viability determined via trypan blue exclusion assay (± SEM, n = 2 independent studies). * $p < 0.05$ less than corresponding value in siSCR transfected cells.

Molecular Pharmacology Fast Forward. Published on May 29, 2009 as DOI: 10.1124/mol.109.056523
This article has not been copyedited and formatted. The final version may differ from this version.

Figure 3. Expression of ceramide synthase 6 (LASS6) modulates the toxicity of sorafenib and vorinostat in SW480 / SW620 colon cancer cells. Panel A. SW480 cells in 8 well chamber slides were transfected with siRNA molecules to knock down expression of acidic sphingomyelinase (ASMase), or transfected with scrambled siRNA molecules. Twenty four h after transfection cells were treated with vehicle or myriocin (1 μM) and after 30 min, cells then exposed to vehicle or to sorafenib + vorinostat. Cells were fixed 6h after exposure and the amount of plasma membrane associated CD95 determined by immunohistochemistry (± SEM, n = 2). Inset lower panel: HEPG2, PANC1, OVCAR and SW480 cells, 24h were transfected with siRNA molecules to knock down expression of LASS6, or transfected with scrambled siRNA molecules; or SW480 cells were transfected with siRNA molecules to knock down expression of ASMase. Twenty four h after transfection cells were isolated and LASS6 / ASMase expression determined. **Panel B.** HEPG2, PANC1, OVCAR and SW480 cells, 24h after plating in 8 well chamber slides were transfected with siRNA molecules to knock down expression of LASS6, or transfected with scrambled siRNA molecules. Twenty four h after transfection cells were treated with vehicle or to sorafenib + valproate or sorafenib + vorinostat. Cells were fixed 6h after exposure and the amount of plasma membrane associated CD95 determined by immunohistochemistry (± SEM, n = 2). **Panel C.** SW480 cells were transfected with siRNA to reduce ASMase protein levels as in *Panel A*. Twenty four h after transfection cells were treated with vehicle or myriocin (1 μM) and after 30 min, cells then exposed to vehicle, sorafenib, vorinostat or both drugs combined. Forty eight hours and 96h after exposure, cells were isolated and stained with trypan blue dye and cell viability determined by visible light microscopy (± SEM, n = 2) * $p < 0.05$ less than corresponding value in siSCR cells; ** $p < 0.05$ less than corresponding value in siASMase cells. **Panel D.** SW620 cells stably transfected with either vector control plasmid of a plasmid to express LASS6, 24h after plating, were exposed to vehicle, sorafenib, vorinostat or both drugs combined. Forty eight hours after exposure, cells were isolated and stained with trypan blue dye and cell viability determined by visible light microscopy (± SEM, n = 2) # $p < 0.05$ greater than corresponding value in empty vector cells. Inset Panel: SW620 cells 24h after plating in 8 well chamber slides as above, and

Molecular Pharmacology Fast Forward. Published on May 29, 2009 as DOI: 10.1124/mol.109.056523
This article has not been copyedited and formatted. The final version may differ from this version.

exposed to vehicle, sorafenib, vorinostat or both drugs combined. Cells were fixed 6h after exposure and the amount of plasma membrane associated CD95 determined by immunohistochemistry (± SEM, n = 2).

Figure 4. Sorafenib and vorinostat interact to cause a CD95-dependent induction of autophagy in HCT116 cells that is cyto-protective. Panel A. HCT116 cells were treated with vehicle, sorafenib, vorinostat or both drugs combined. Cells were isolated 6h and 24h after drug treatment and lysates subjected to SDS PAGE and immunoblotting against the proteins indicated in the Figure panel. Data are from a representative of three independent studies. **Panel B.** HCT116 cells in 8 well chamber slides were transfected with a vector control plasmid (CMV) or a plasmid to express dominant negative PERK and all cells transfected with a plasmid to express LC3-GFP. Twenty four h after infection, cells were treated with vehicle, sorafenib, vorinostat or both drugs combined. Six h after drug exposure cells were visualized at 40X using an Axiovert 200 fluorescent microscope under fluorescent light using the FITC filter. The mean number of autophagic vesicles per cell from random fields of 40 cells were counted (± SEM, n = 3). Inset Panel: cells transfected with vector control (CMV) or a plasmid to express dominant negative PERK (but not LC3-GFP) were isolated 6h after drug exposure and lysates subjected to SDS PAGE and immunoblotting to determine LC3 expression and processing; PERK phosphorylation, and JNK1/2 phosphorylation (a representative n = 3). **Panel C.** HCT116 cells in 8 well chambered glass slides were transfected with siRNA molecules to knock down expression of CD95, ATG5 or Beclin1. In parallel, cells were co-transfected with a plasmid to express LC3-GFP. Twenty four h after transfection, cells were treated with vehicle, sorafenib, vorinostat or both drugs combined. Six hours after drug exposure, cells were visualized at 40X using an Axiovert 200 fluorescent microscope under fluorescent light using the FITC filter. The mean number of autophagic vesicles per cell from random fields of 40 cells were counted (± SEM, n = 3). * $p < 0.05$ less than corresponding value in siSCR transfected cells. Inset microscopy Panel: representative microscopic images taken from each of the treatment conditions in CD95 studies. Inset blotting Panel: siRNA treatment knocks down of Beclin1 or ATG5 in HCT116 cells 24h after transfection. **Panel D.** HCT116 cells in 8 well chambered glass slides were transfected with siRNA molecules to knock down expression of Beclin1. Twenty four h after transfection, cells were treated with vehicle,

Molecular Pharmacology Fast Forward. Published on May 29, 2009 as DOI: 10.1124/mol.109.056523
This article has not been copyedited and formatted. The final version may differ from this version.

sorafenib, vorinostat or both drugs combined. Forty eight h after exposure, cells were isolated and viability determined via trypan blue exclusion assay (± SEM, n = 3 independent studies). # $p < 0.05$ greater than corresponding value in siSCR transfected cells.

Figure 5. Sorafenib and vorinostat toxicity in HCT116 cells is enhanced by inhibition of the JNK1/2 pathway. Panel A. Upper blot: HCT116 cells were treated with either vehicle or with sorafenib and vorinostat. Six h – 24h after drug exposure cells were isolated and subjected to SDS PAGE and immunoblotting to determine the phosphorylation of p38 MAPK and JNK1/2. Data are from a representative of 3 independent studies. **Lower Graph:** HCT116 cells were, as indicated, infected with recombinant adenoviruses. Thirty minutes prior to drug exposure cells were treated as indicated with vehicle (DMSO) or the JNK inhibitory peptide (JNK-IP, 10 μM). Twenty four h after infection, cells were treated with vehicle, sorafenib, vorinostat or both drugs together. Ninety six hours after exposure, cells were isolated and stained with Annexin V – propidium iodide and cell viability determined by flow cytometry (± SEM, n = 3) * $p < 0.05$ less than corresponding value in CMV vector cells; # $p < 0.05$ greater than corresponding value in CMV vector cells. **Panel B. Upper blot:** HCT116 cells 24h after plating were transfected with: a scrambled siRNA (siSCR) or an siRNA to knock down CD95 expression. Twenty four h after infection, cells were treated with vehicle or with sorafenib and vorinostat. Six h after drug exposure cells were isolated and lysates subjected to SDS PAGE and immunoblotting to determine the phosphorylation status of PERK and of JNK1/2. Data are from a representative of 2-3 independent studies. **Lower Graph:** HCT116 cells in 8 well chamber slides were transfected with a plasmid to express LC3-GFP. Thirty minutes prior to drug exposure cells were treated as indicated with vehicle or the JNK inhibitory peptide (JNK-IP, 10 μM). Twenty four h after infection, cells were treated with vehicle, sorafenib, vorinostat or both drugs combined. Six h after drug exposure cells were visualized at 40X using an Axiovert 200 fluorescent microscope under fluorescent light using the FITC filter. The mean number of autophagic vesicles per cell from random fields of 40 cells were counted (± SEM, n = 3). **Panel C.** HCT116 cells were treated with vehicle or JNK inhibitory peptide (10 μM). Cells were then treated

Molecular Pharmacology Fast Forward. Published on May 29, 2009 as DOI: 10.1124/mol.109.056523
This article has not been copyedited and formatted. The final version may differ from this version.

with vehicle or with sorafenib and sodium valproate. Cells were isolated 6h after exposure and BCL-2 immunoprecipitated from cell lysates. Immunoprecipitates were subjected to SDS PAGE and blotting to determine association of Beclin1 and BCL-2 in the samples (n = 2).

Figure 6. Transient modulation of ERK1/2 activity, and not AKT activity, regulates sorafenib + vorinostat toxicity in HCT116 cells. Panel A. Upper blot: HCT116 cells 24h after plating were treated with either vehicle or with sorafenib + vorinostat. Twenty four h – 96h after drug exposure cells were isolated and subjected to SDS PAGE and immunoblotting to determine the phosphorylation of ERK1/2 and AKT (S473). Data are from a representative of 3 independent studies. **Lower Graph:** HCT116 cells 24h after plating were, as indicated, infected with recombinant adenoviruses. Twenty four h after infection, cells were treated with vehicle, sorafenib, vorinostat or both drugs together. Forty eight hours after exposure, cells were isolated and stained with Annexin V – propidium iodide and cell viability determined by flow cytometry (± SEM, n = 3) # $p < 0.05$ greater than corresponding value in CMV vector cells; ## $p < 0.05$ greater than corresponding value in dnMEK1 cells. **Panel B.** HCT116 cells were, as indicated, infected with recombinant adenoviruses. Twenty four h after infection, cells were treated with vehicle, sorafenib, vorinostat or both drugs together. Ninety six hours after exposure, cells were isolated and stained with Annexin V – propidium iodide and cell viability determined by flow cytometry (± SEM, n = 3) * $p < 0.05$ less than corresponding value in CMV vector cells. Upper inset blots: the phosphorylation of ERK1/2 and AKT (S473) were measured in cells expressing MEK1EE and activated AKT, respectively, 24h after virus infection.

Molecular Pharmacology Fast Forward. Published on May 29, 2009 as DOI: 10.1124/mol.109.056523
This article has not been copyedited and formatted. The final version may differ from this version.

Table 1. Sorafenib and vorinostat synergize in colony formation assays to kill colon cancer cells. Colon cancer (HCT116, SW480) cells were treated 12h after plating as single cells (250-1500 cells/well) in sextuplicate with vehicle (VEH, DMSO), sorafenib (Sor., 3.0-6.0 μM) or vorinostat (Vor. 250-500 nM), or with both drugs combined, as indicated at a fixed concentration ratio to perform median dose effect analyses for the determination of synergy. After drug exposure (48h), the media was changed and cells cultured in drug free media for an additional 10-14 days. Cells were fixed, stained with crystal violet and colonies of > 50 cells / colony counted. Colony formation data were entered into the Calcusyn program and combination index (CI) values determined. A CI value of less than 1.00 indicates synergy; a CI value of greater than 1.00 indicates antagonism.

HCT116			SW480		
Sor (μM)	Vor (μM)	CI	Sor (μM)	Vor (μM)	CI
3.0	0.250	0.46	3.0	0.250	0.57
4.5	0.375	0.59	4.5	0.375	0.59
6.0	0.500	0.66	6.0	0.500	0.49

Molecular Pharmacology Fast Forward. Published on May 29, 2009 as DOI: 10.1124/mol.109.056523
This article has not been copyedited and formatted. The final version may differ from this version.

Table 2. Sorafenib and sodium valproate synergize in colony formation assays to kill colon cancer cells.

Colon cancer (HCT116, SW480) cells were treated 12h after plating as single cells (250-1500 cells/well) in sextuplicate with vehicle (VEH, DMSO), sorafenib (Sor., 2.0-9.0 μM) or sodium valproate (Val. 0.33-1.5 mM), or with both drugs combined, as indicated at a fixed concentration ratio to perform median dose effect analyses for the determination of synergy. After drug exposure (48h), the media was changed and cells cultured in drug free media for an additional 10-14 days. Cells were fixed, stained with crystal violet and colonies of > 50 cells / colony counted. Colony formation data were entered into the Calcusyn program and combination index (CI) values determined. A CI value of less than 1.00 indicates synergy; a CI value of greater than 1.00 indicates antagonism.

Sor. (μM)	Val. (mM)	CI (HCT116)
3.0	0.50	0.65
4.5	0.75	0.66
6.0	1.00	0.64
7.5	1.25	0.49
9.0	1.50	0.48

Sor. (μM)	Val. (mM)	CI (SW480)
2.0	0.33	0.57
3.0	0.50	0.68
4.0	0.66	0.74

Molecular Pharmacology Fast Forward. Published on May 29, 2009 as DOI: 10.1124/mol.109.056523
This article has not been copyedited and formatted. The final version may differ from this version.

Table 3. Sorafenib and sodium valproate synergize in colony formation assays to kill rhabdomyosarcoma cells. Rhabdomyosarcoma (Rh41) cells were treated 12h after plating as single cells (250-1500 cells/well) in sextuplicate with vehicle (VEH, DMSO), sorafenib (Sor., 2.0-9.0 μM) or sodium valproate (Val. 0.33-1.5 mM), or with both drugs combined, as indicated at a fixed concentration ratio to perform median dose effect analyses for the determination of synergy. After drug exposure (48h), the media was changed and cells cultured in drug free media for an additional 10-14 days. Cells were fixed, stained with crystal violet and colonies of > 50 cells / colony counted. Colony formation data were entered into the Calcusyn program and combination index (CI) values determined. A CI value of less than 1.00 indicates synergy; a CI value of greater than 1.00 indicates antagonism.

Rh41		
Sor. (μM)	Val. (mM)	CI
3.0	0.50	0.82
4.5	0.75	0.73
6.0	1.00	0.40
7.5	1.25	0.31
9.0	1.50	0.12

Figure 1A

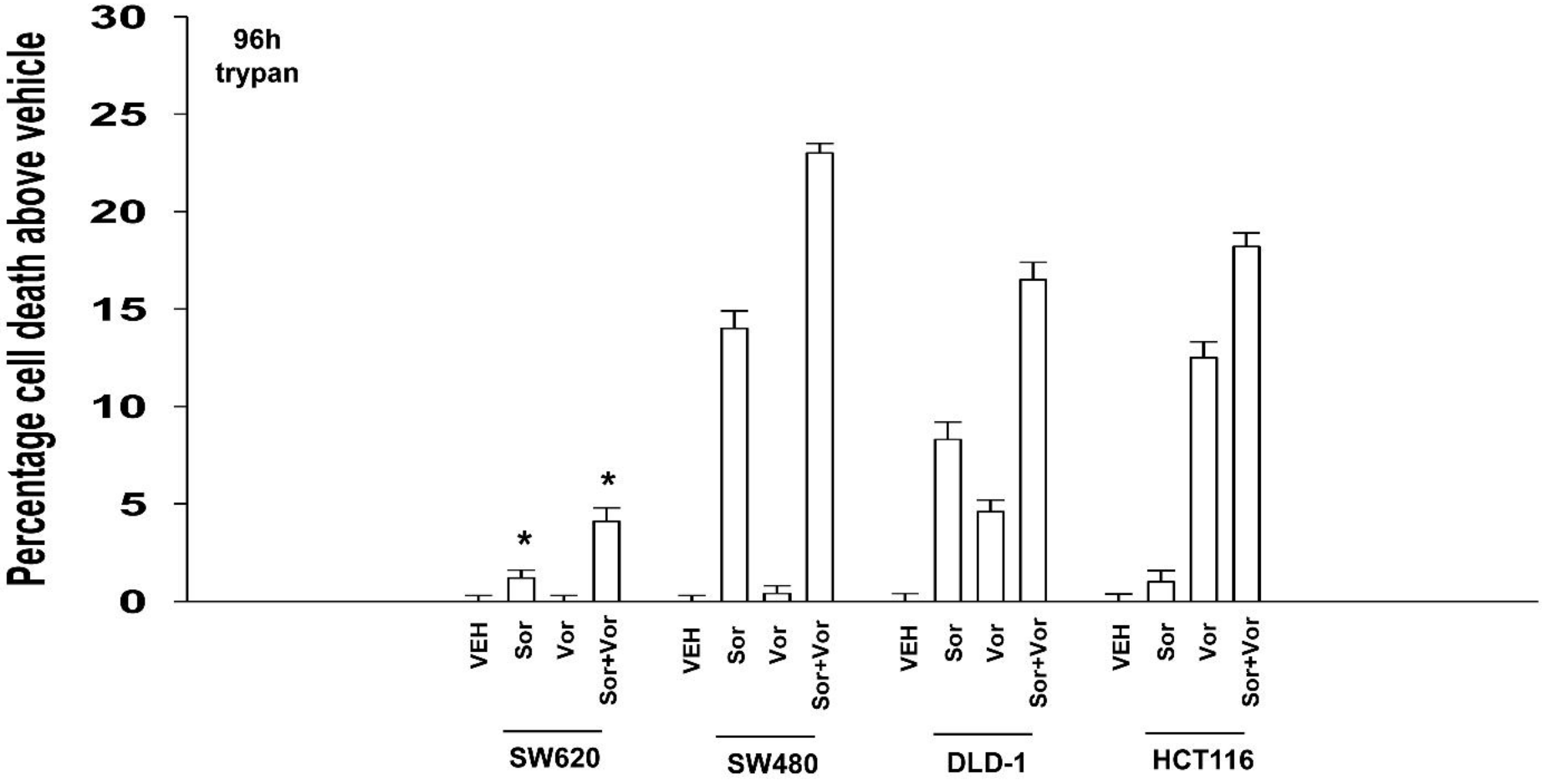
Percentage cell death above vehicle
30
25
20
15
10
5
0
96h
trypan
*
*
VEH
Sor
Vor
Sor+Vor
SW620
SW480
DLD-1
HCT116

Figure 1B

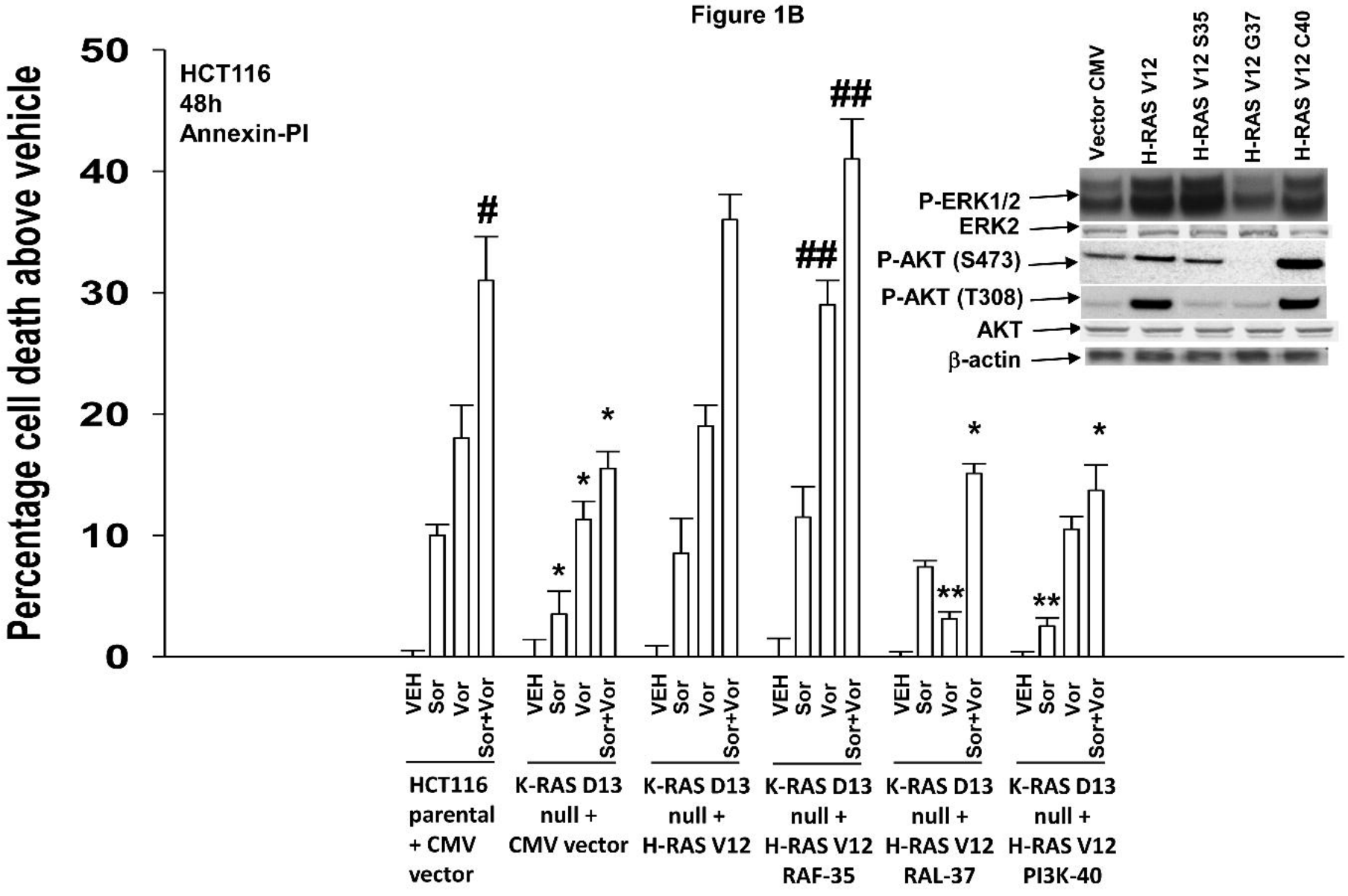
Percentage cell death above vehicle
50
40
30
20
10
0
HCT116
48h
Annexin-PI
#
##
##
*
*
*
*
*
**
**
Vector CMV
H-RAS V12
H-RAS V12 S35
H-RAS V12 G37
H-RAS V12 C40
P-ERK1/2
ERK2
P-AKT (S473)
P-AKT (T308)
AKT
β-actin
VEH
Sor
Vor
Sor+Vor
HCT116 parental + CMV vector
K-RAS D13 null + CMV vector
K-RAS D13 null + H-RAS V12
K-RAS D13 null + H-RAS V12 RAF-35
K-RAS D13 null + H-RAS V12 RAL-37
K-RAS D13 null + H-RAS V12 PI3K-40

Figure 1C

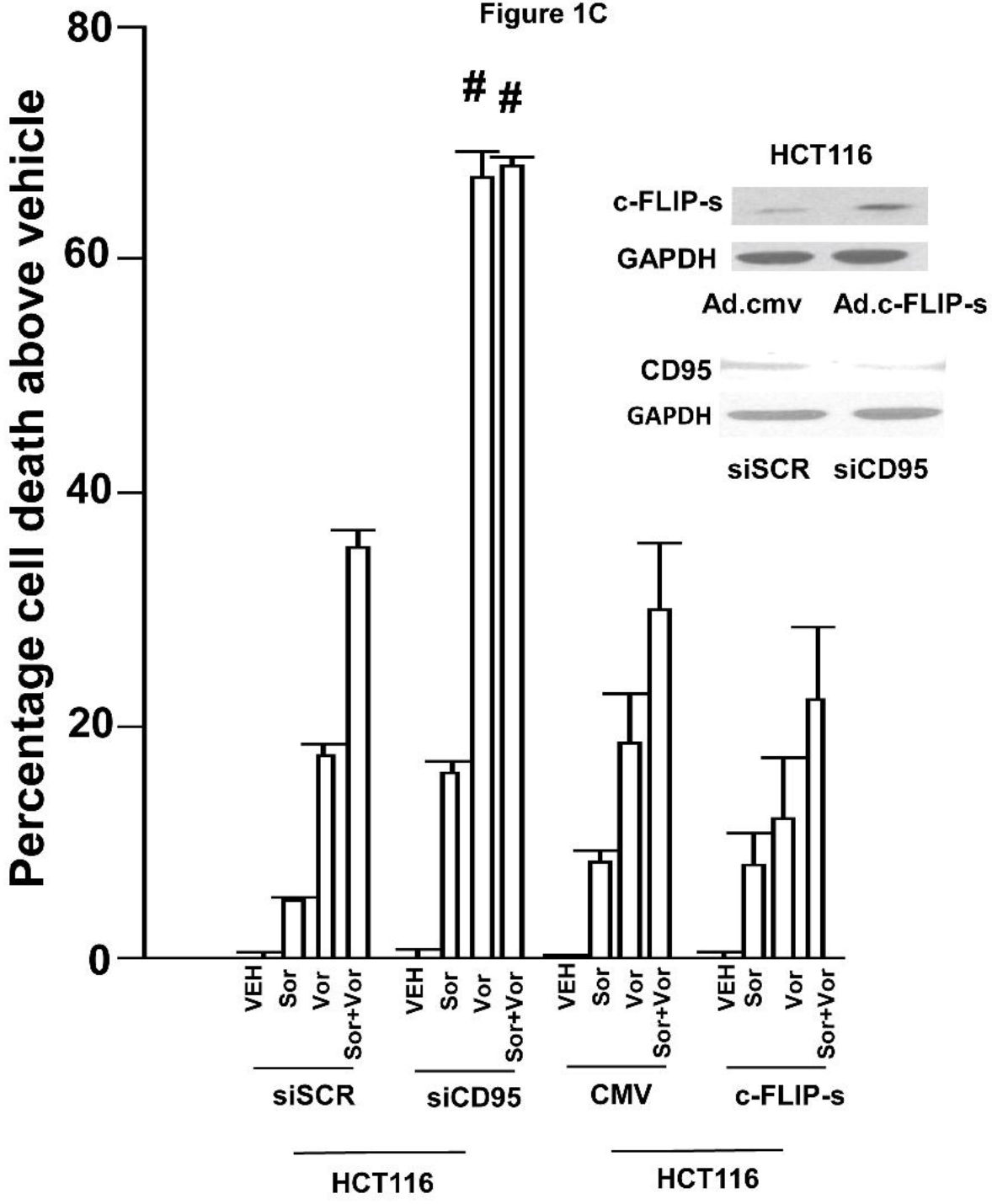
Percentage cell death above vehicle
80
60
40
20
0
# #
HCT116
c-FLIP-s
GAPDH
Ad.cmv
Ad.c-FLIP-s
CD95
GAPDH
siSCR
siCD95
VEH
Sor
Vor
Sor+Vor
siSCR
siCD95
CMV
c-FLIP-s
HCT116
HCT116

Figure 1D

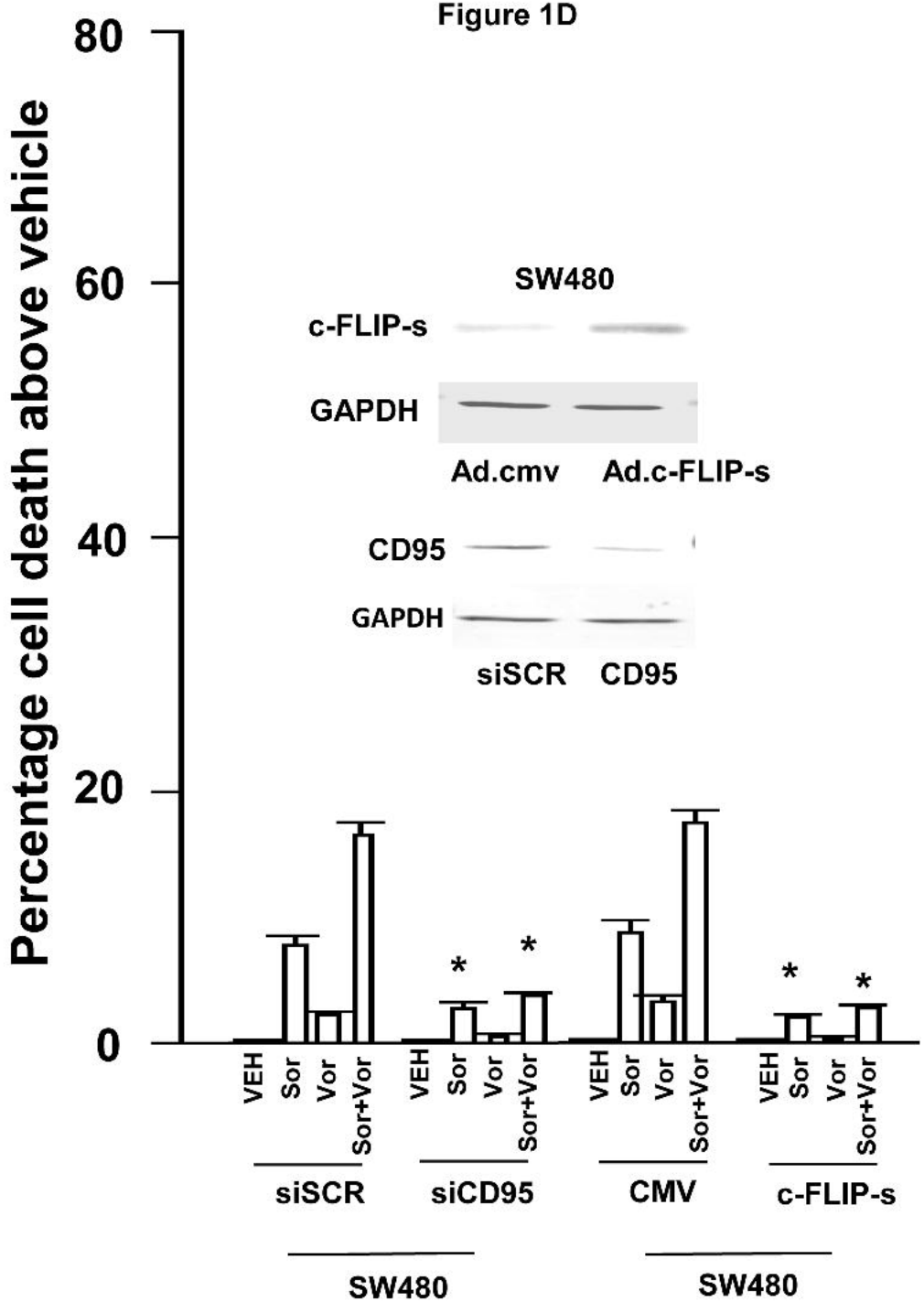
Percentage cell death above vehicle
80
60
40
20
0
SW480
c-FLIP-s
GAPDH
Ad.cmv
Ad.c-FLIP-s
CD95
GAPDH
siSCR
CD95
VEH
Sor
Vor
Sor+Vor
*
siSCR
siCD95
CMV
c-FLIP-s
SW480
SW480

Figure 1E

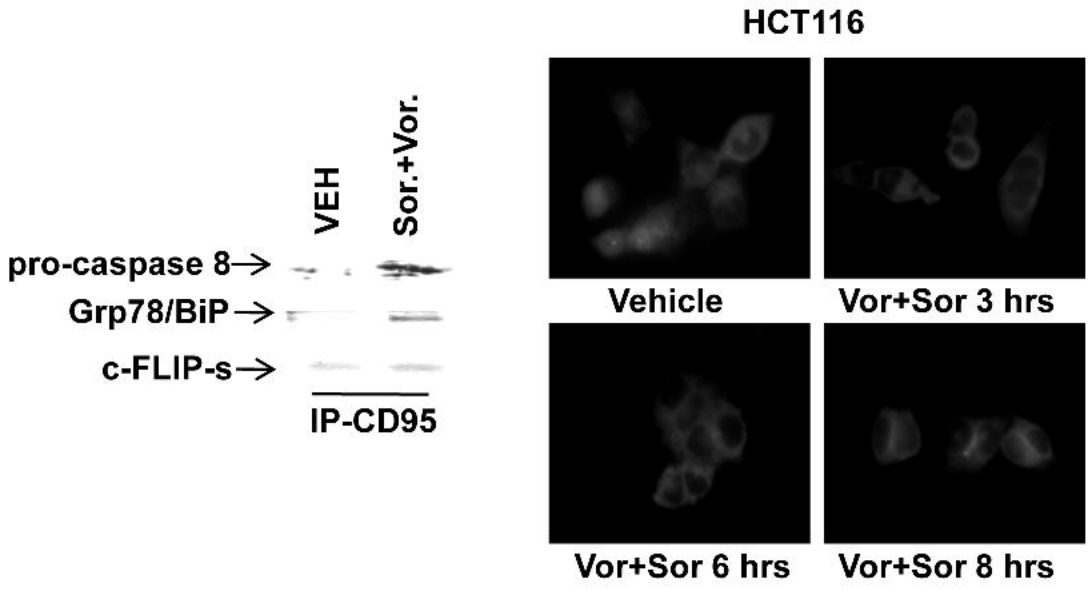
HCT116
VEH
Sor.+Vor.
pro-caspase 8
Grp78/BiP
c-FLIP-s
IP-CD95
Vehicle
Vor+Sor 3 hrs
Vor+Sor 6 hrs
Vor+Sor 8 hrs

Figure 1F

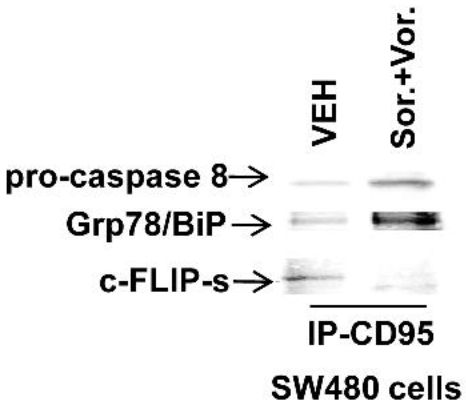
VEH
Sor.+Vor.
pro-caspase 8
Grp78/BiP
c-FLIP-s
IP-CD95
SW480 cells

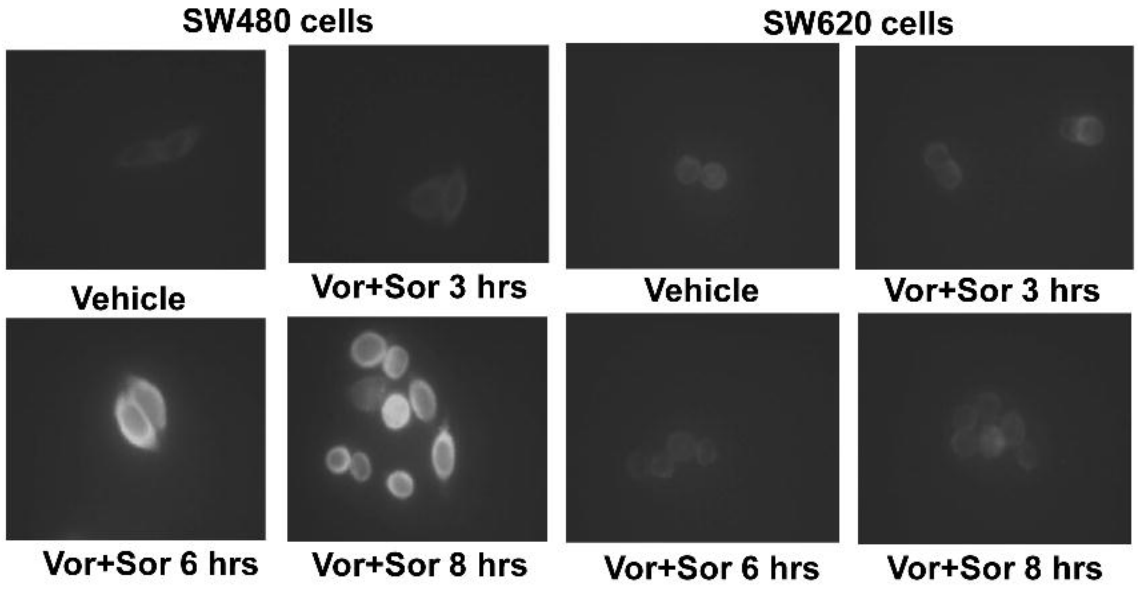
SW480 cells
SW620 cells
Vehicle
Vor+Sor 3 hrs
Vehicle
Vor+Sor 3 hrs
Vor+Sor 6 hrs
Vor+Sor 8 hrs
Vor+Sor 6 hrs
Vor+Sor 8 hrs

Figure 2A

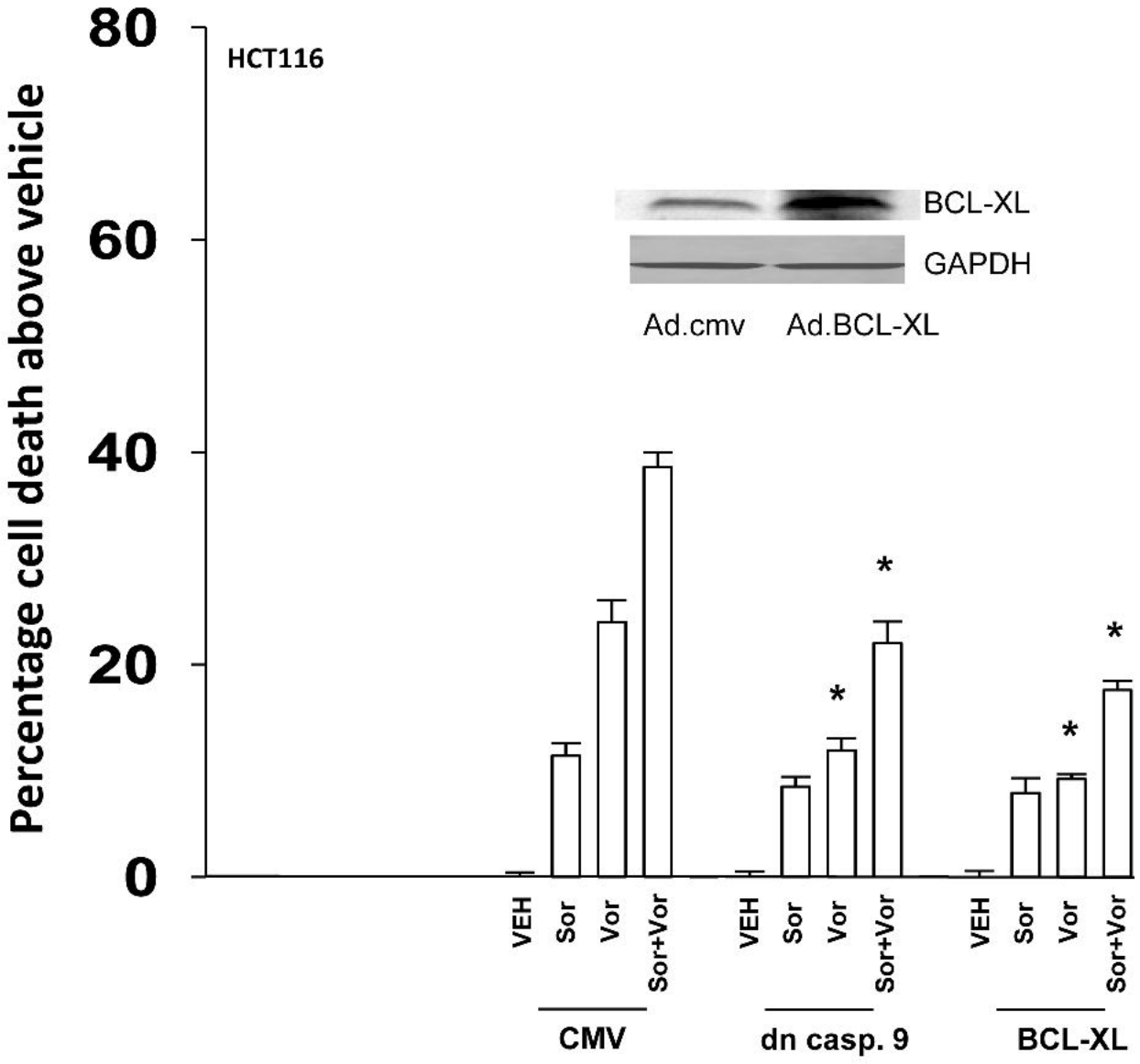
HCT116
Percentage cell death above vehicle
80
60
40
20
0
BCL-XL
GAPDH
Ad.cmv
Ad.BCL-XL
VEH
Sor
Vor
Sor+Vor
CMV
dn casp. 9
BCL-XL
*

Figure 2B

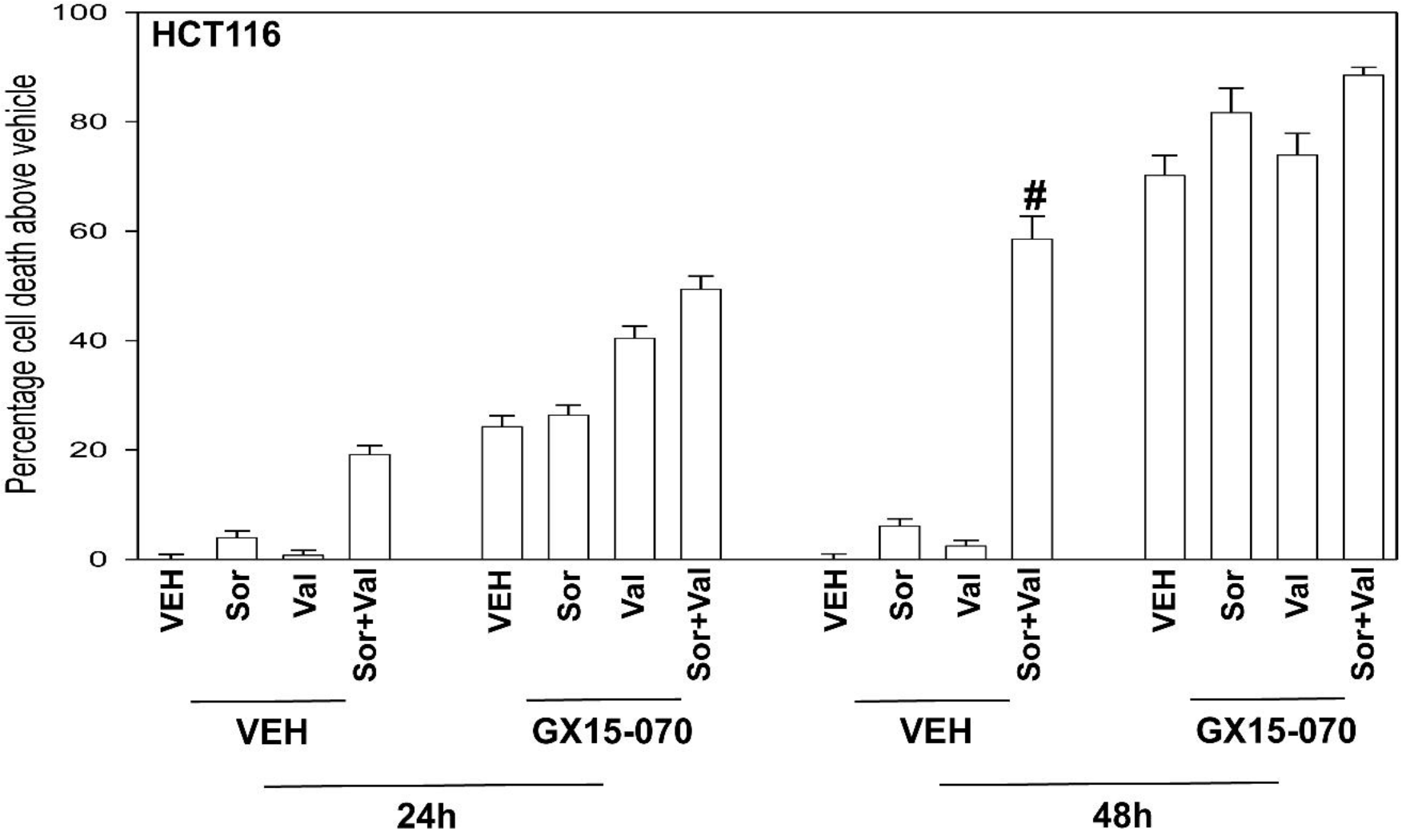
HCT116
Percentage cell death above vehicle
100
80
60
40
20
0
#
VEH
Sor
Val
Sor+Val
VEH
Sor
Val
Sor+Val
VEH
Sor
Val
Sor+Val
VEH
Sor
Val
Sor+Val
VEH
GX15-070
VEH
GX15-070
24h
48h

Figure 2C

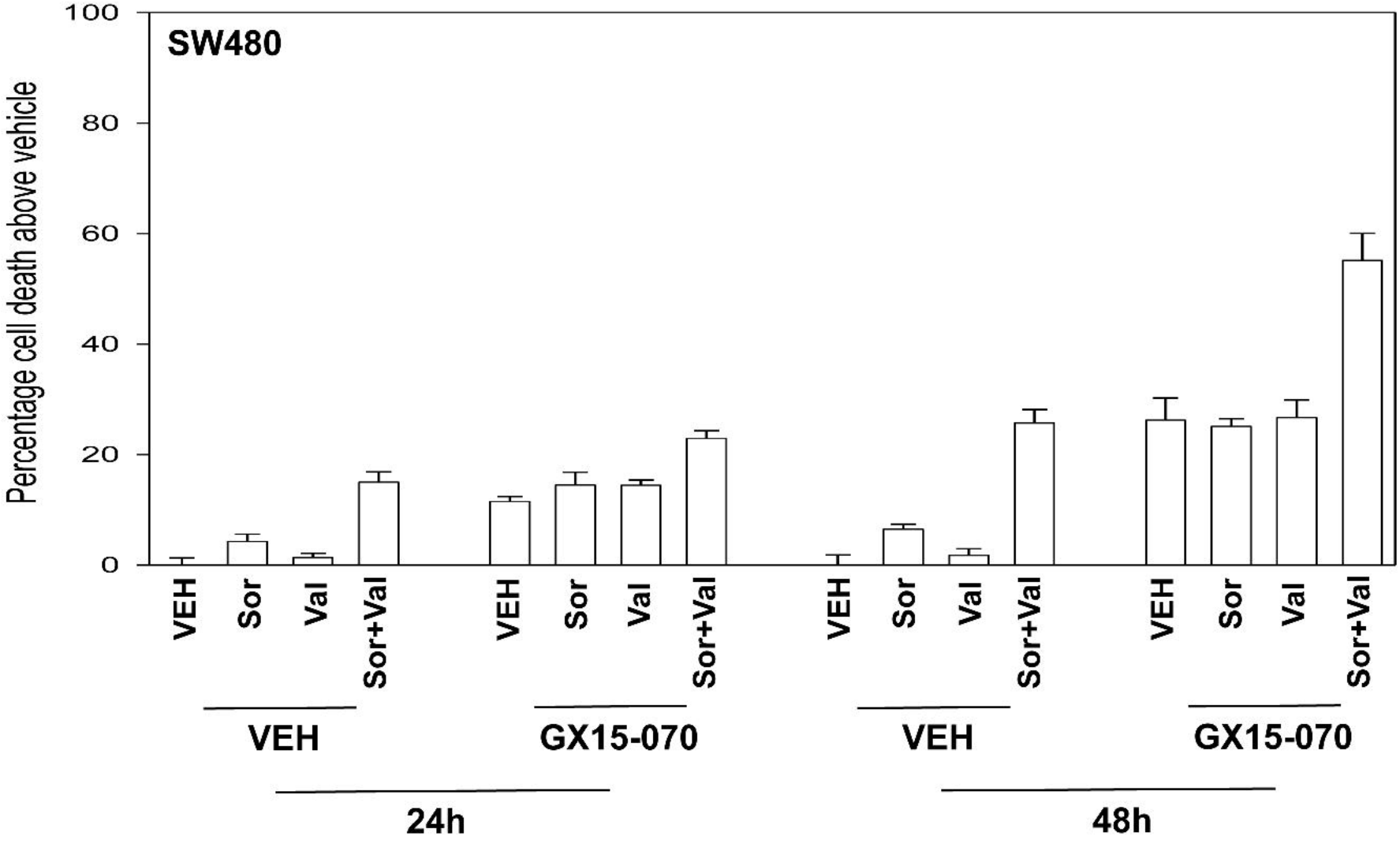
SW480
Percentage cell death above vehicle
100
80
60
40
20
0
VEH
Sor
Val
Sor+Val
VEH
Sor
Val
Sor+Val
VEH
Sor
Val
Sor+Val
VEH
Sor
Val
Sor+Val
VEH
GX15-070
VEH
GX15-070
24h
48h

Figure 2D

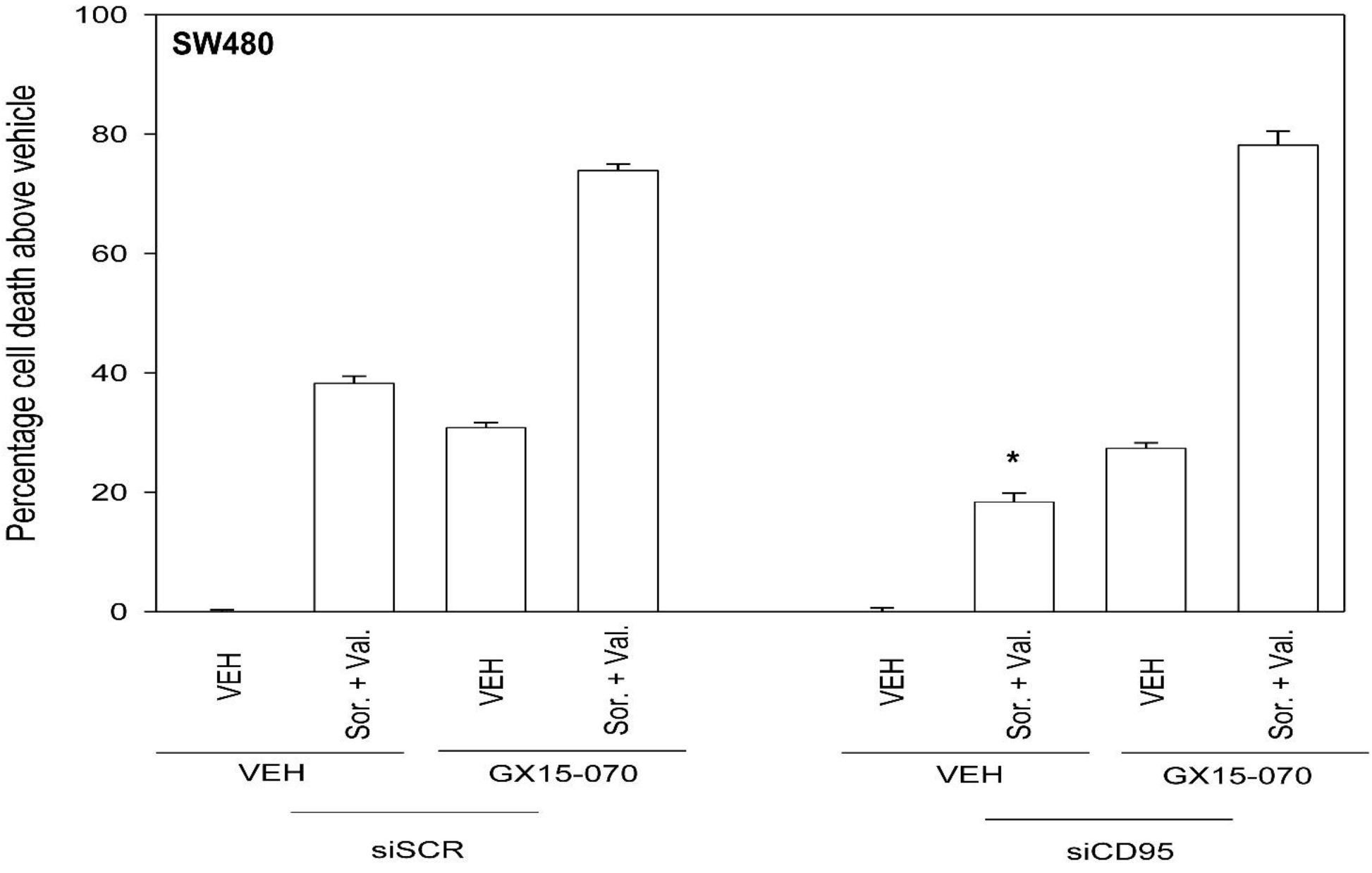
SW480
Percentage cell death above vehicle
100
80
60
40
20
0
*
VEH
Sor. + Val.
VEH
Sor. + Val.
VEH
Sor. + Val.
VEH
Sor. + Val.
VEH
GX15-070
VEH
GX15-070
siSCR
siCD95

Figure 2E

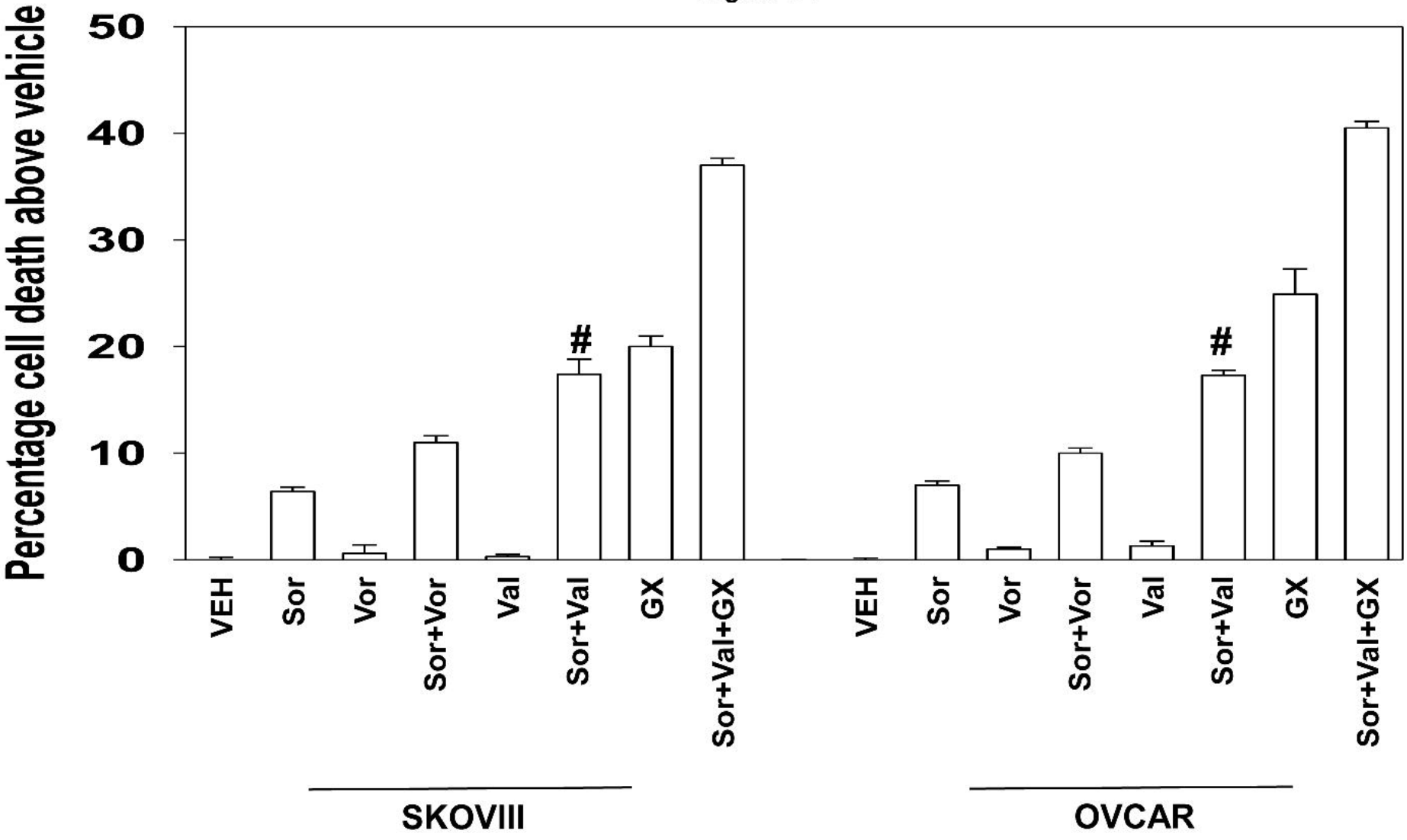
Percentage cell death above vehicle
50
40
30
20
10
0
#
#
VEH
Sor
Vor
Sor+Vor
Val
Sor+Val
GX
Sor+Val+GX
VEH
Sor
Vor
Sor+Vor
Val
Sor+Val
GX
Sor+Val+GX
SKOVIII
OVCAR

Figure 2F

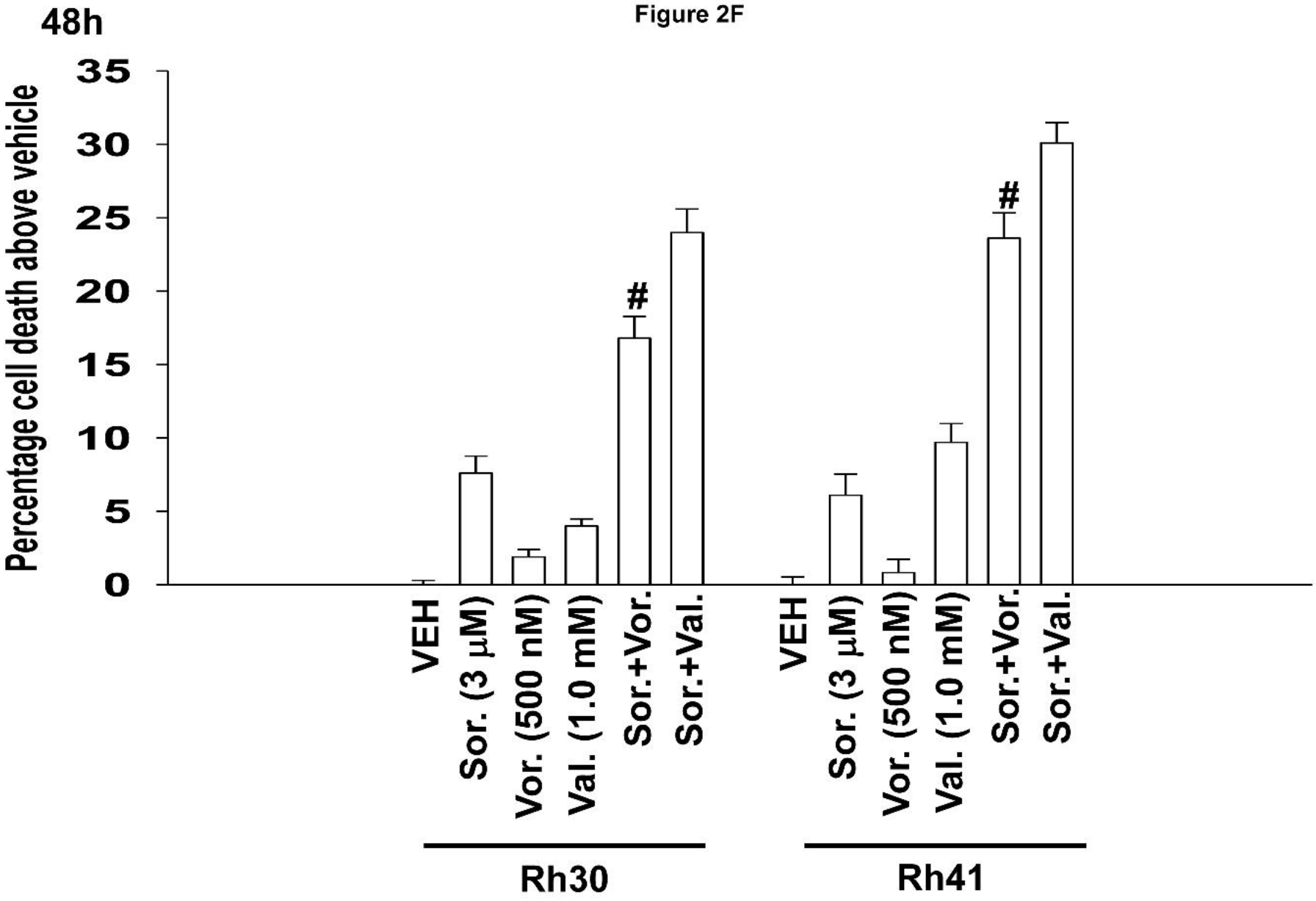
48h
Percentage cell death above vehicle
35
30
25
20
15
10
5
0
#
#
VEH
Sor. (3 μM)
Vor. (500 nM)
Val. (1.0 mM)
Sor.+Vor.
Sor.+Val.
VEH
Sor. (3 μM)
Vor. (500 nM)
Val. (1.0 mM)
Sor.+Vor.
Sor.+Val.
Rh30
Rh41

Figure 2G

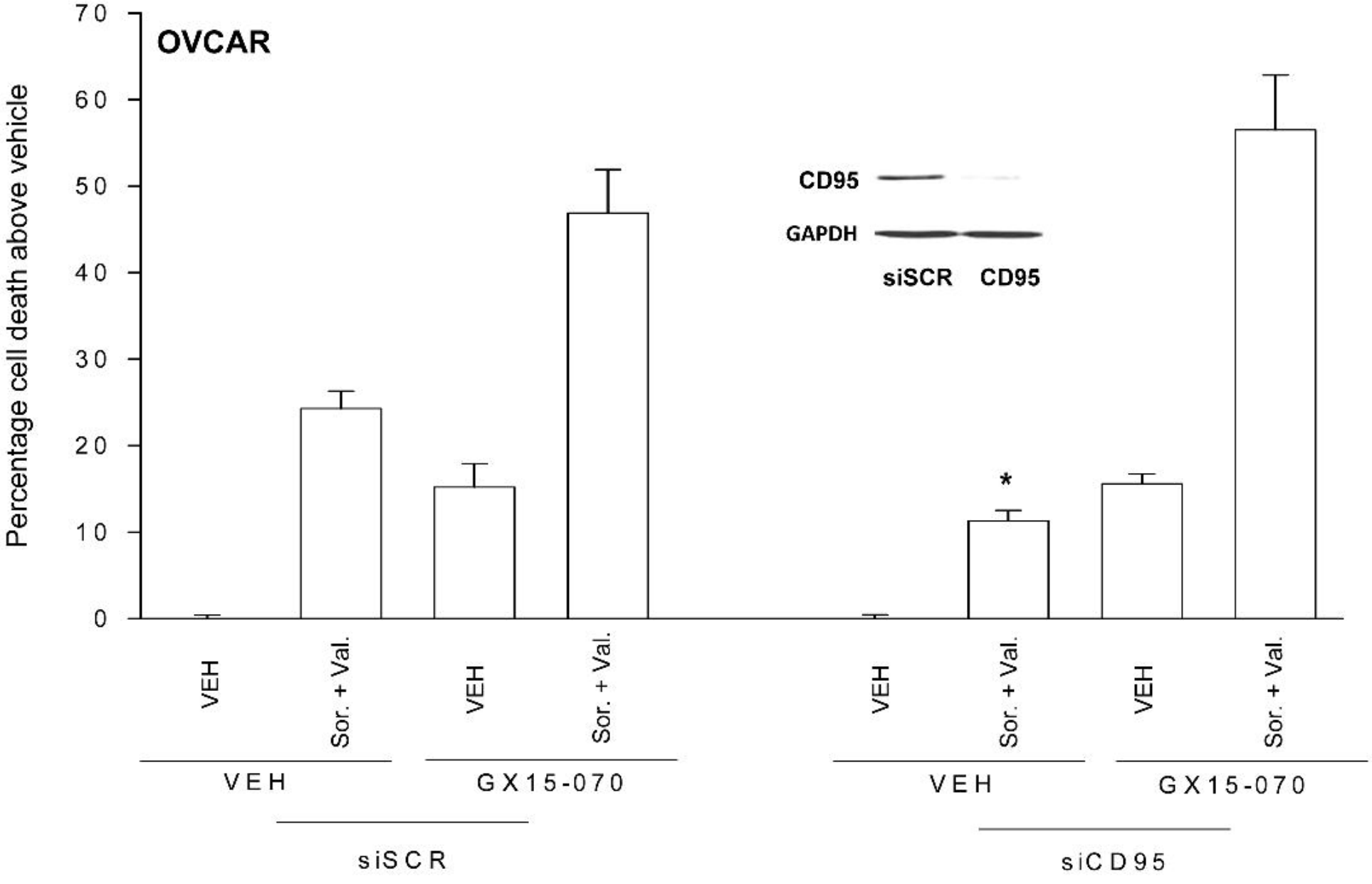
OVCAR
Percentage cell death above vehicle
70
60
50
40
30
20
10
0
CD95
GAPDH
siSCR
CD95
*
VEH
Sor. + Val.
VEH
Sor. + Val.
VEH
Sor. + Val.
VEH
Sor. + Val.
VEH
GX15-070
VEH
GX15-070
siSCR
siCD95

Figure 2H

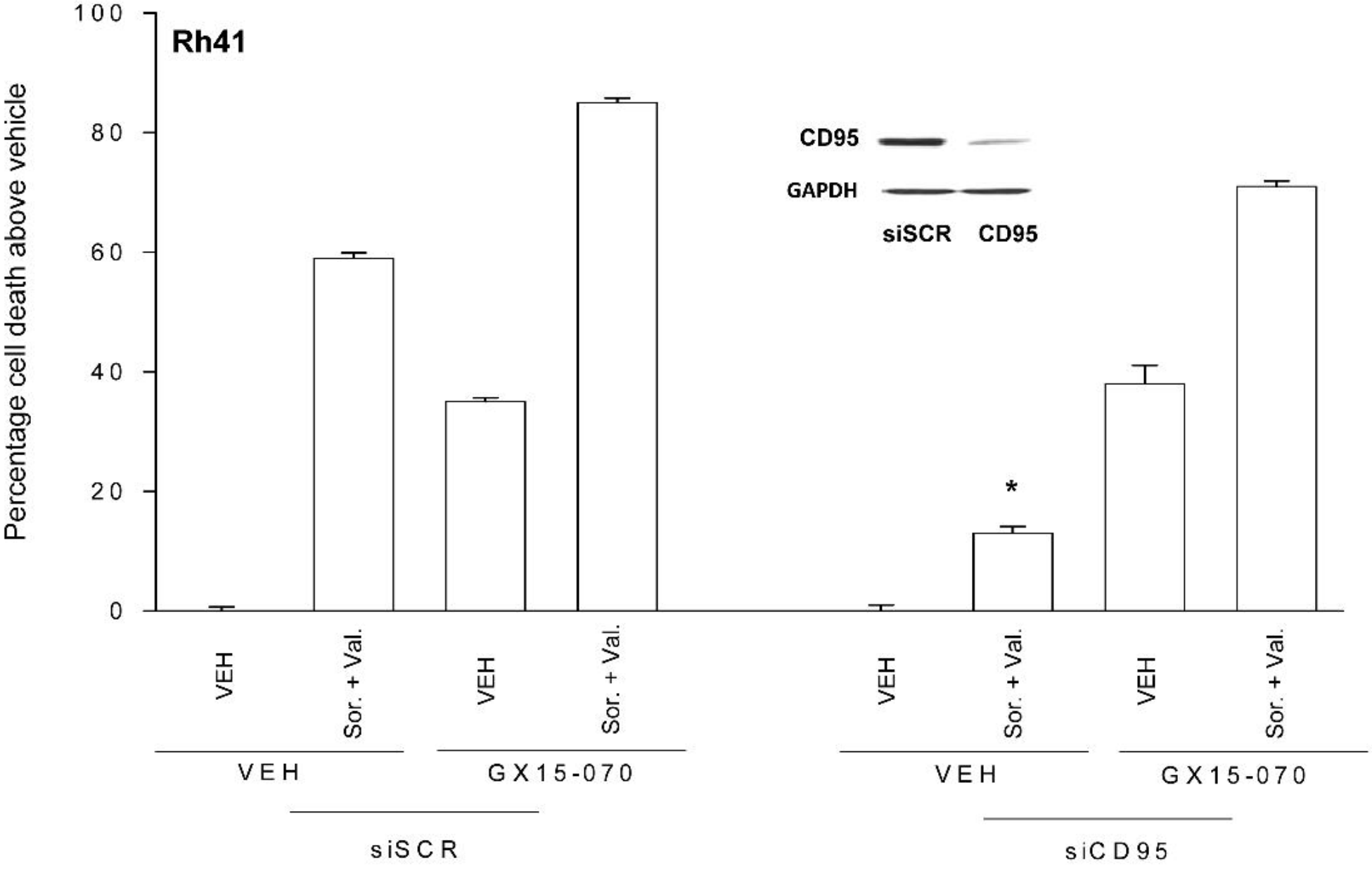
Rh41
Percentage cell death above vehicle
100
80
60
40
20
0
CD95
GAPDH
siSCR
CD95
*
VEH
Sor. + Val.
VEH
Sor. + Val.
VEH
Sor. + Val.
VEH
Sor. + Val.
VEH
GX15-070
VEH
GX15-070
siSCR
siCD95

Figure 3A

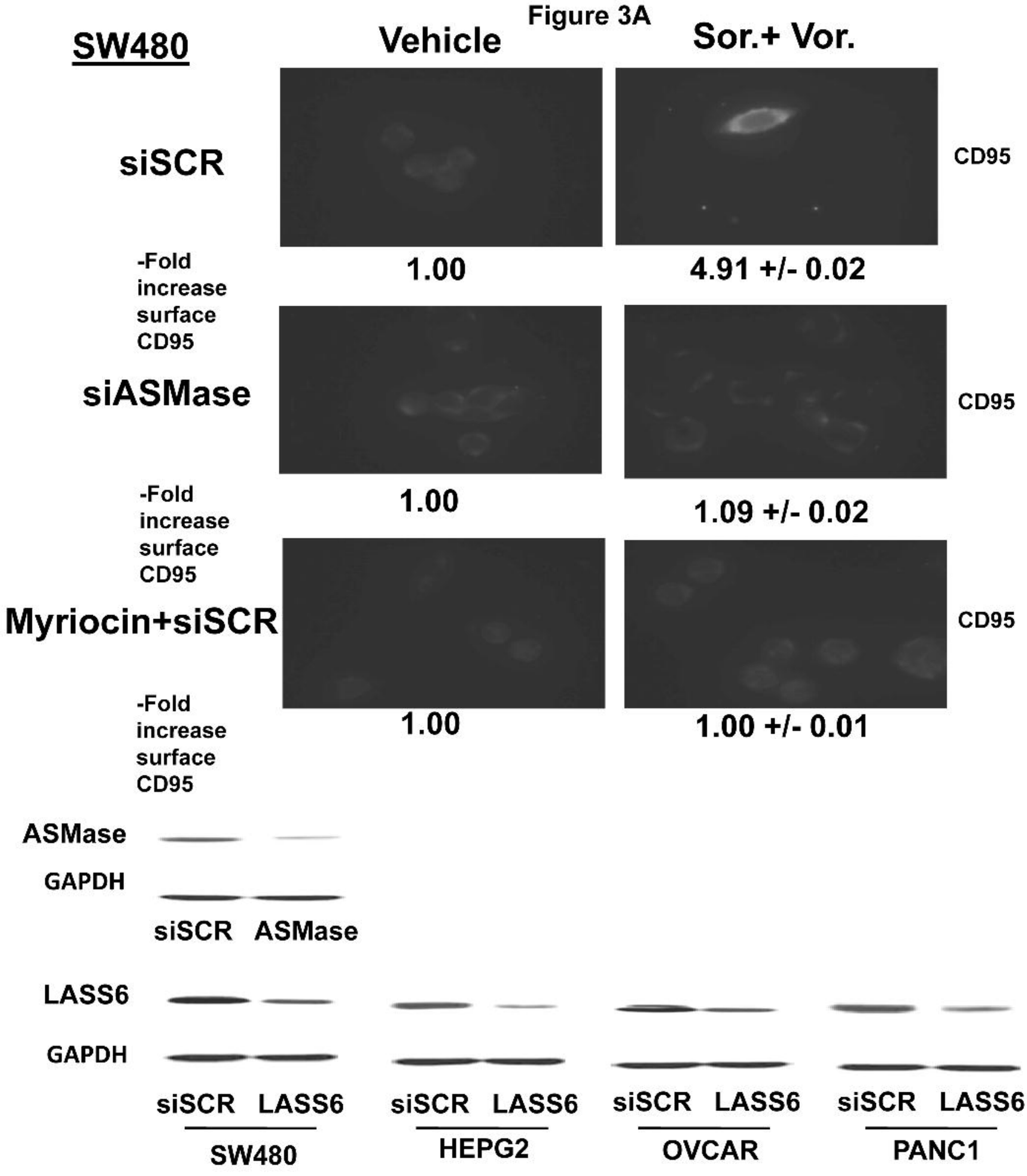
SW480
Vehicle
Sor.+ Vor.
siSCR
CD95
-Fold increase surface CD95
1.00
4.91 +/- 0.02
siASMase
CD95
-Fold increase surface CD95
1.00
1.09 +/- 0.02
Myriocin+siSCR
CD95
-Fold increase surface CD95
1.00
1.00 +/- 0.01
ASMase
GAPDH
siSCR ASMase
LASS6
GAPDH
siSCR LASS6
siSCR LASS6
siSCR LASS6
siSCR LASS6
SW480
HEPG2
OVCAR
PANC1

Figure 3B

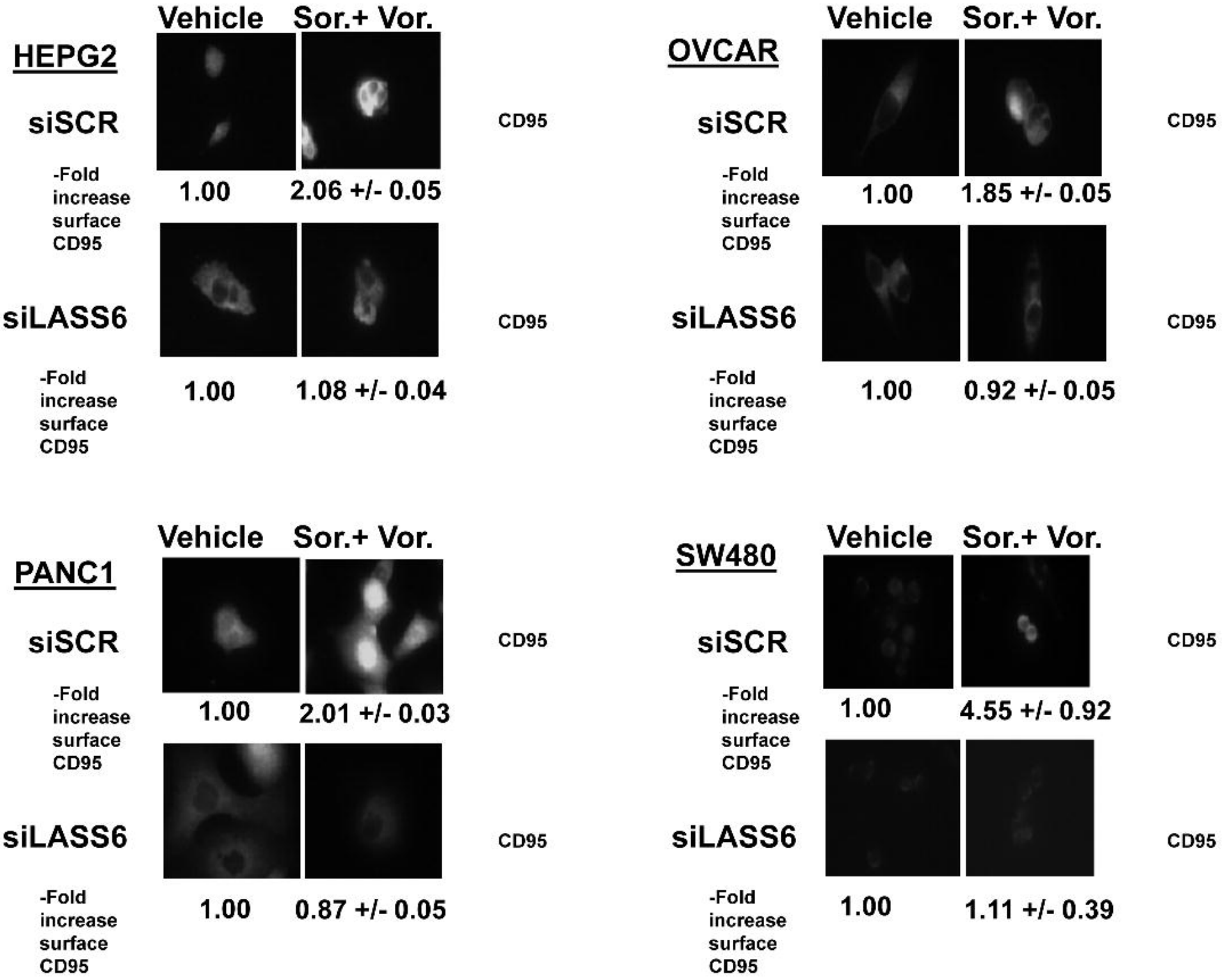
Vehicle
Sor.+ Vor.
HEPG2
siSCR
CD95
-Fold increase surface CD95
1.00
2.06 +/- 0.05
siLASS6
CD95
-Fold increase surface CD95
1.00
1.08 +/- 0.04
OVCAR
siSCR
CD95
-Fold increase surface CD95
1.00
1.85 +/- 0.05
siLASS6
CD95
-Fold increase surface CD95
1.00
0.92 +/- 0.05
PANC1
siSCR
CD95
-Fold increase surface CD95
1.00
2.01 +/- 0.03
siLASS6
CD95
-Fold increase surface CD95
1.00
0.87 +/- 0.05
SW480
siSCR
CD95
-Fold increase surface CD95
1.00
4.55 +/- 0.92
siLASS6
CD95
-Fold increase surface CD95
1.00
1.11 +/- 0.39

Figure 3C

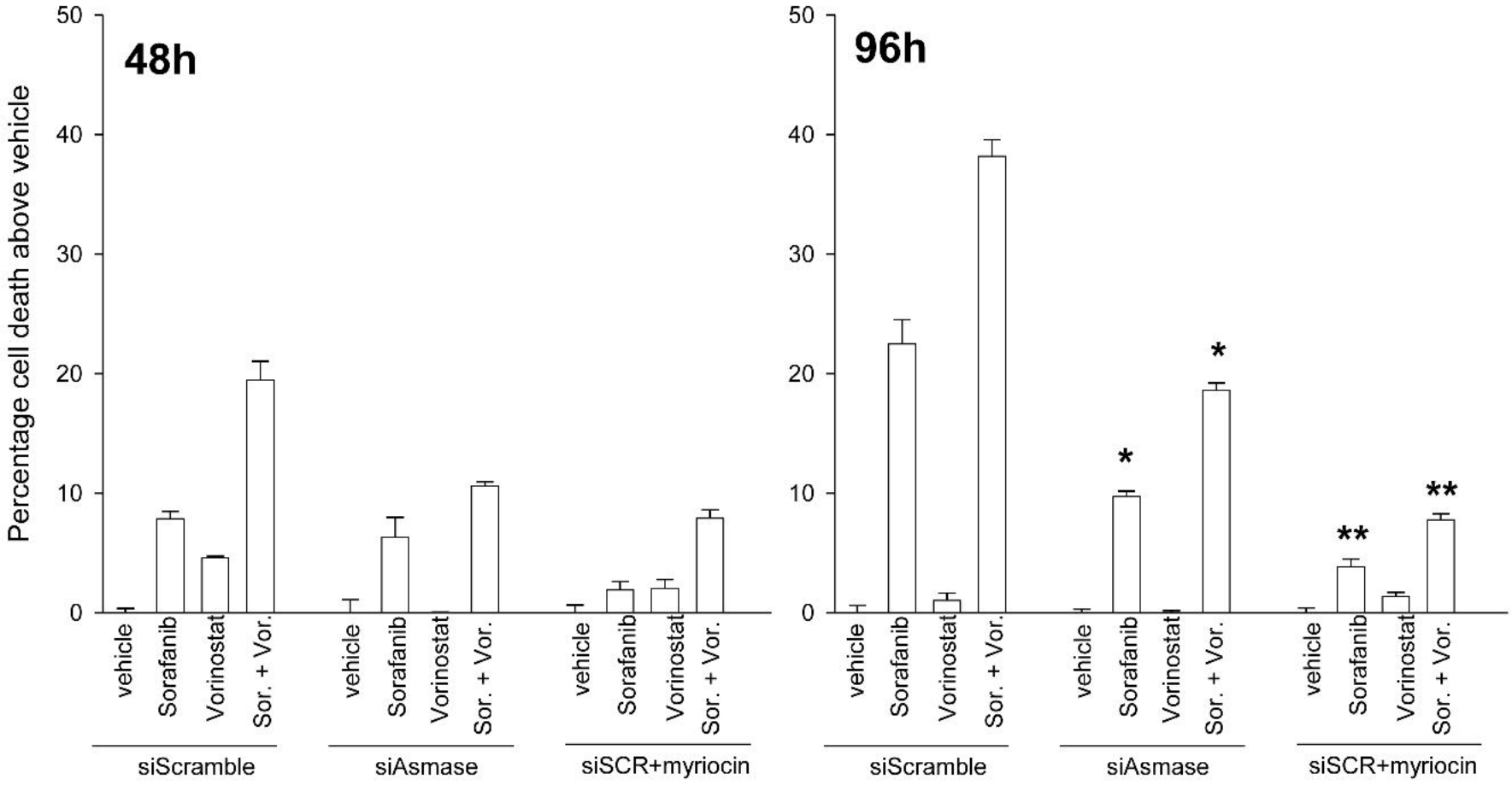
48h
96h
Percentage cell death above vehicle
50
40
30
20
10
0
vehicle
Sorafanib
Vorinostat
Sor. + Vor.
siScramble
siAsmase
siSCR+myriocin
*
**

Figure 3D

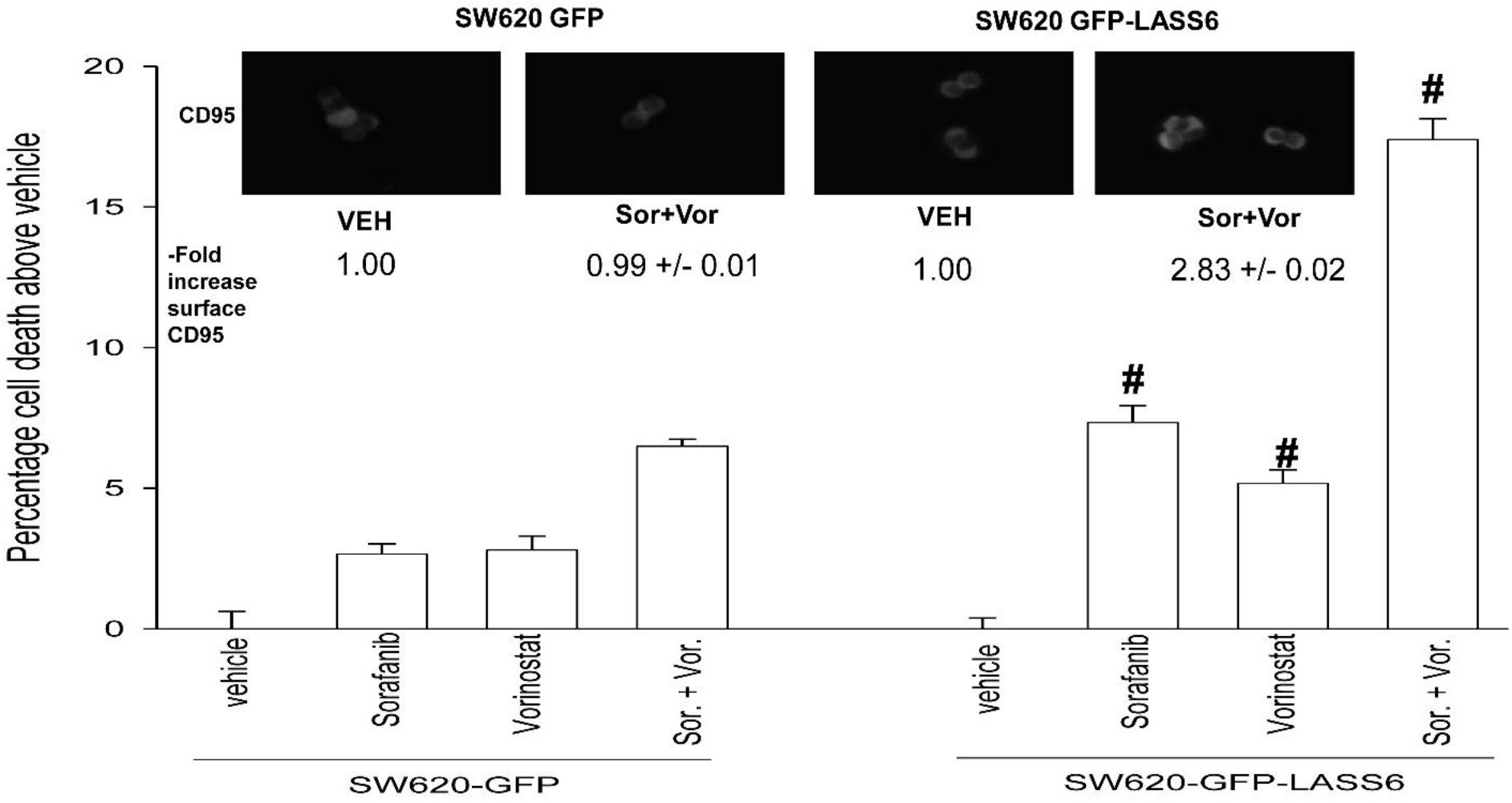
SW620 GFP
SW620 GFP-LASS6
CD95
VEH
Sor+Vor
VEH
Sor+Vor
-Fold increase surface CD95
1.00
0.99 +/- 0.01
1.00
2.83 +/- 0.02
Percentage cell death above vehicle
20
15
10
5
0
#
#
#
vehicle
Sorafanib
Vorinostat
Sor. + Vor.
vehicle
Sorafanib
Vorinostat
Sor. + Vor.
SW620-GFP
SW620-GFP-LASS6

Figure 4A

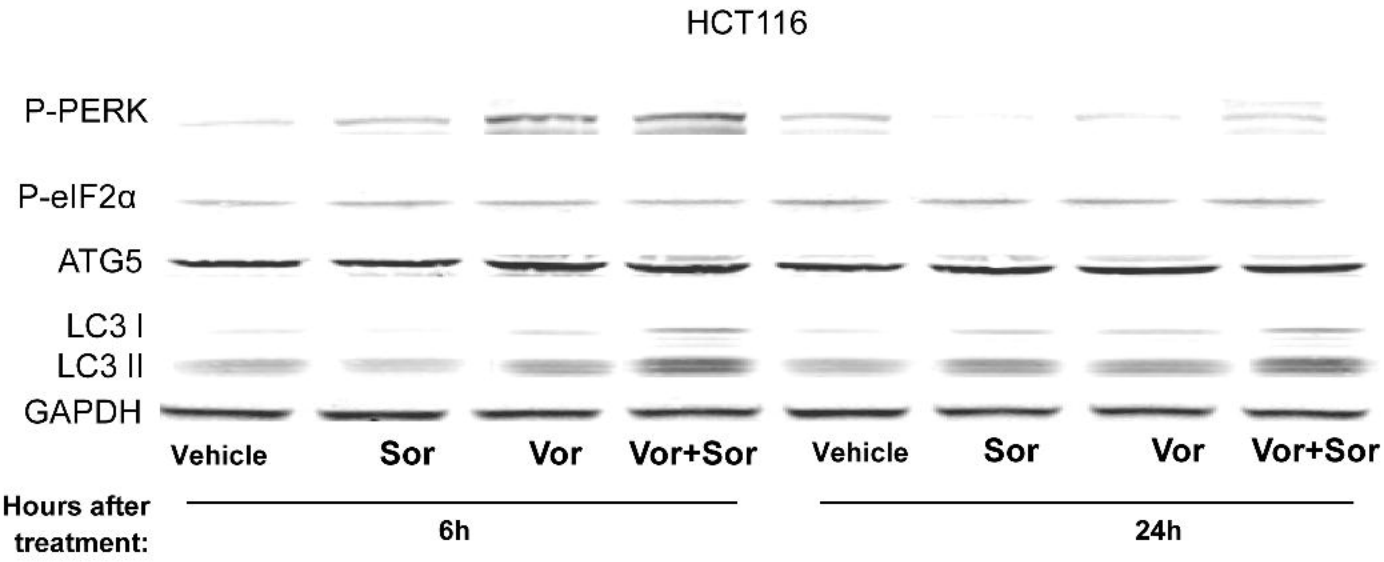
HCT116
P-PERK
P-eIF2α
ATG5
LC3 I
LC3 II
GAPDH
Vehicle
Sor
Vor
Vor+Sor
Vehicle
Sor
Vor
Vor+Sor
Hours after treatment:
6h
24h

Figure 4B

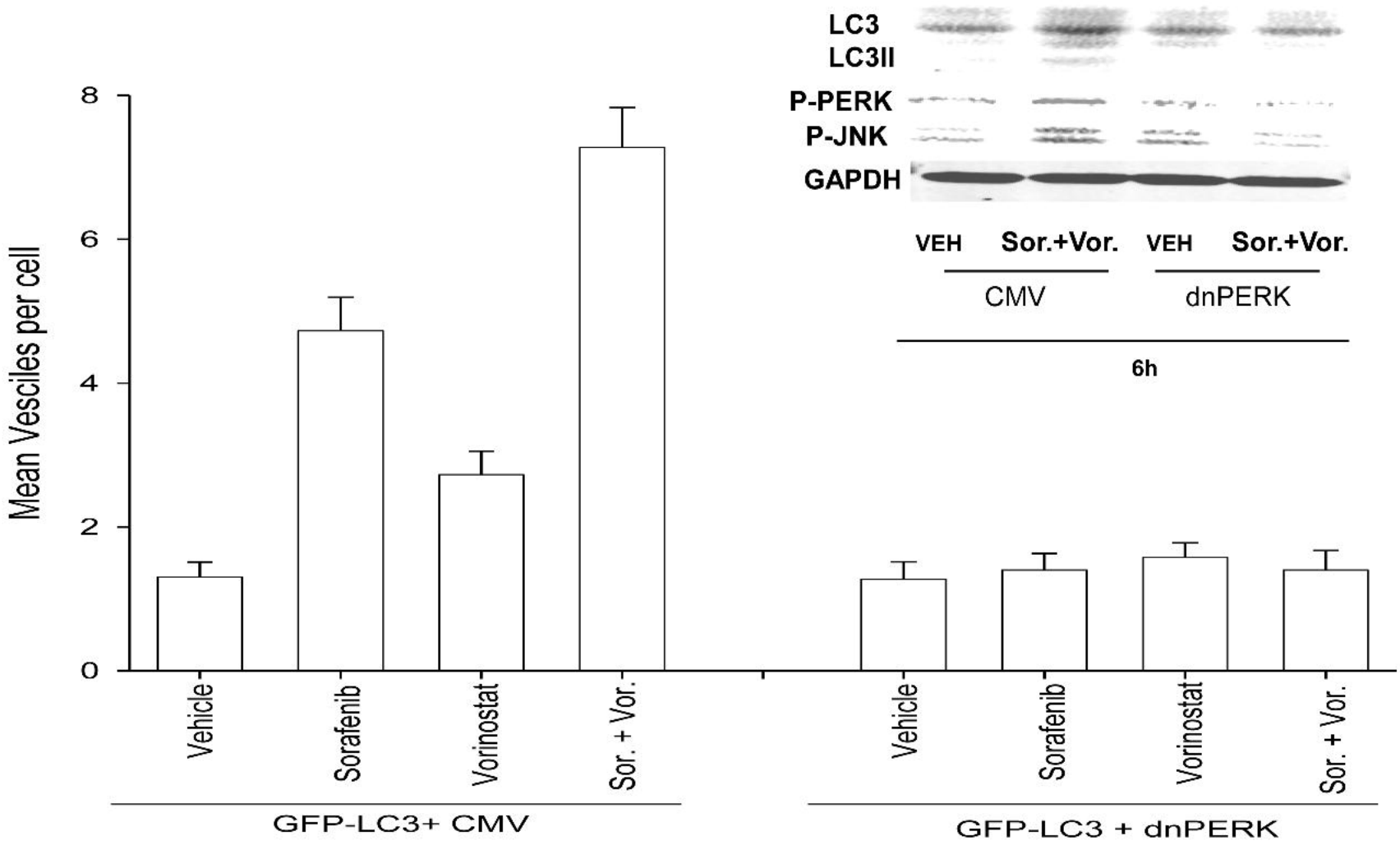
LC3
LC3II
P-PERK
P-JNK
GAPDH
VEH
Sor.+Vor.
VEH
Sor.+Vor.
CMV
dnPERK
6h
Mean Vesciles per cell
0
2
4
6
8
Vehicle
Sorafenib
Vorinostat
Sor. + Vor.
GFP-LC3+ CMV
Vehicle
Sorafenib
Vorinostat
Sor. + Vor.
GFP-LC3 + dnPERK

Figure 4C

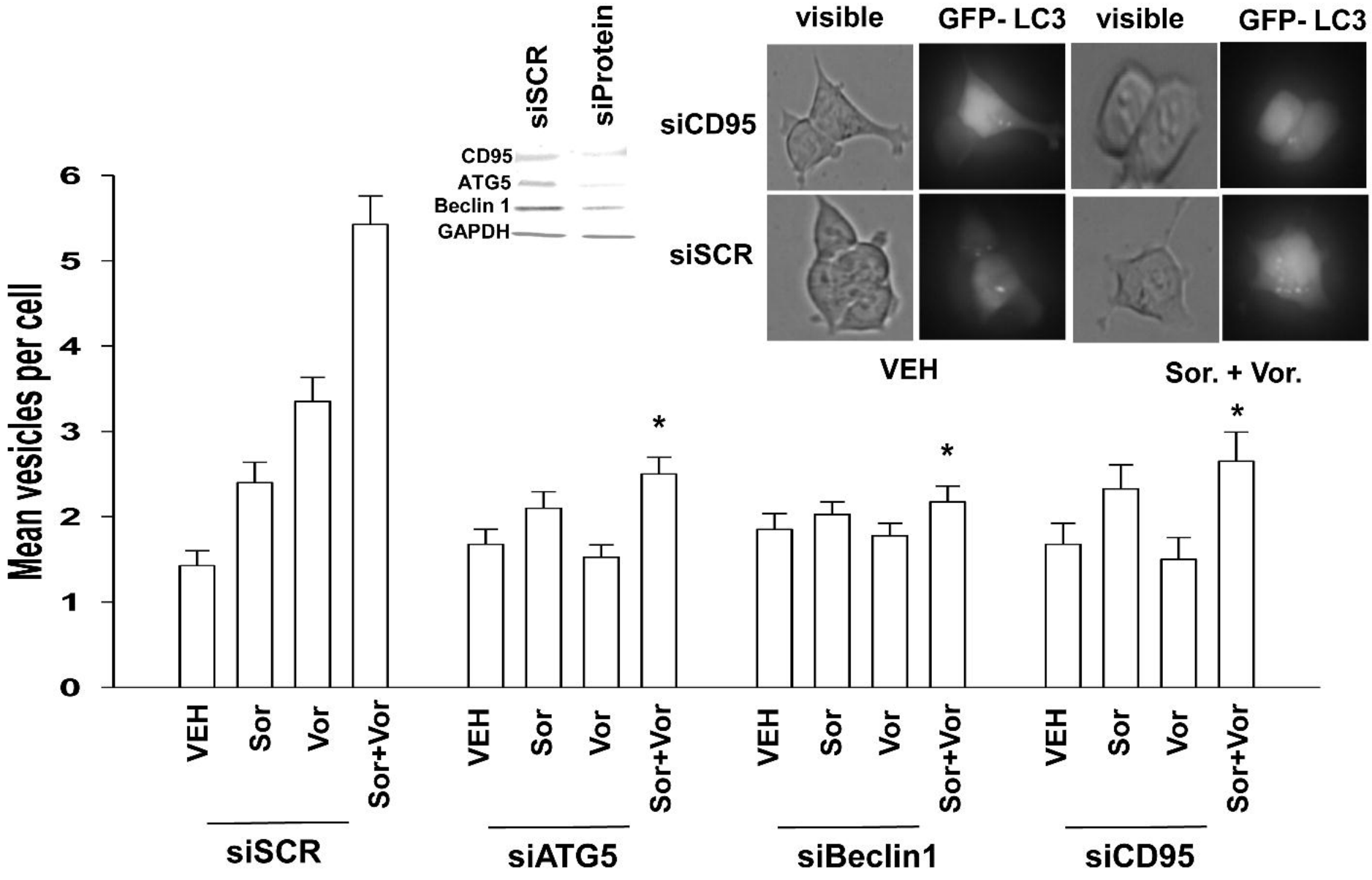
visible
GFP- LC3
visible
GFP- LC3
siCD95
siSCR
VEH
Sor. + Vor.
siSCR
siProtein
CD95
ATG5
Beclin 1
GAPDH
Mean vesicles per cell
0
1
2
3
4
5
6
*
*
*
VEH
Sor
Vor
Sor+Vor
siSCR
siATG5
siBeclin1
siCD95

Figure 4D

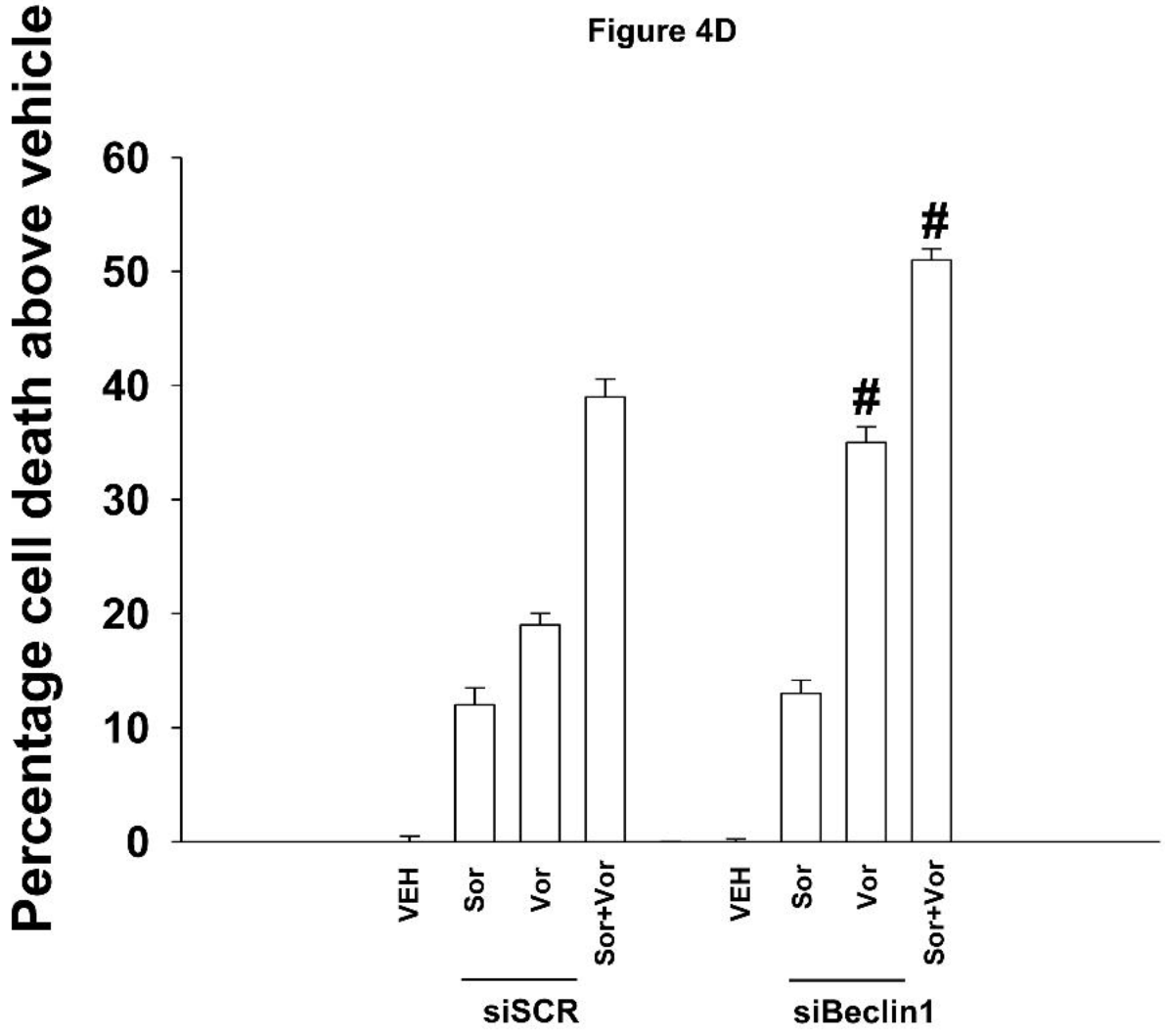
Percentage cell death above vehicle
60
50
40
30
20
10
0
#
#
VEH
Sor
Vor
Sor+Vor
VEH
Sor
Vor
Sor+Vor
siSCR
siBeclin1

Figure 5A

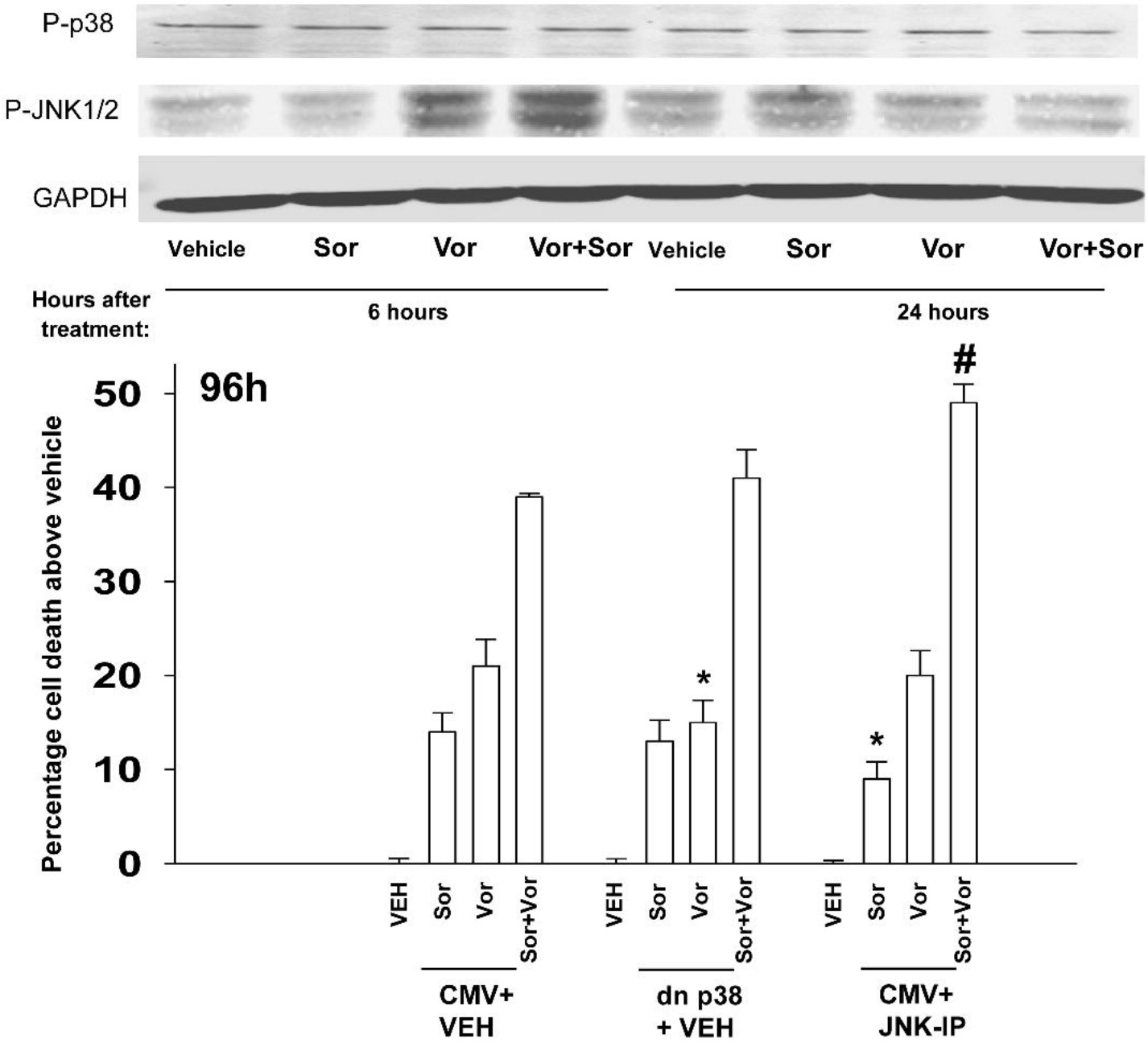
P-p38
P-JNK1/2
GAPDH
Vehicle
Sor
Vor
Vor+Sor
Vehicle
Sor
Vor
Vor+Sor
Hours after treatment:
6 hours
24 hours
96h
Percentage cell death above vehicle
50
40
30
20
10
0
#
*
*
VEH
Sor
Vor
Sor+Vor
VEH
Sor
Vor
Sor+Vor
VEH
Sor
Vor
Sor+Vor
CMV+ VEH
dn p38 + VEH
CMV+ JNK-IP

Figure 5B

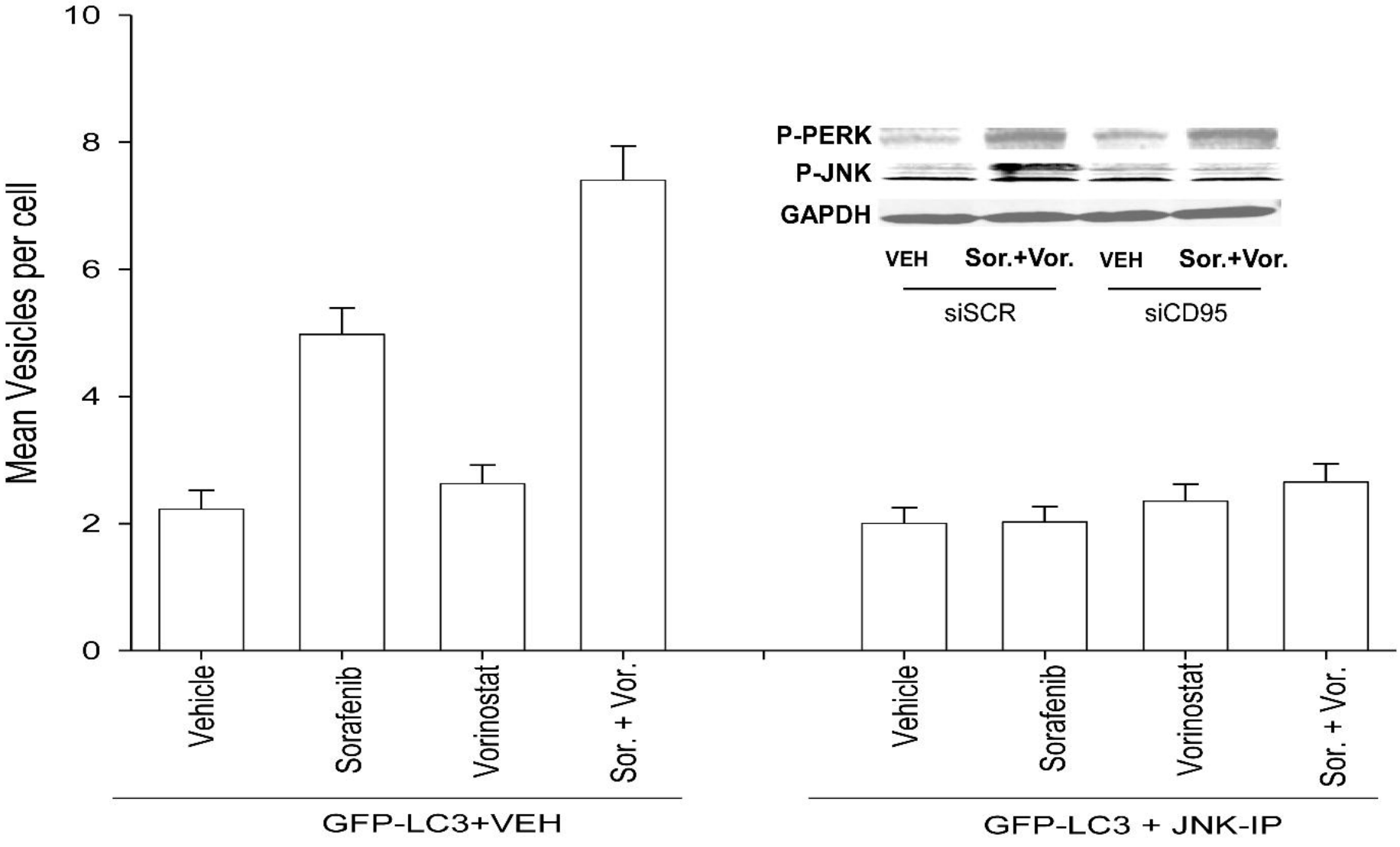
Mean Vesicles per cell
10
8
6
4
2
0
Vehicle
Sorafenib
Vorinostat
Sor. + Vor.
GFP-LC3+VEH
Vehicle
Sorafenib
Vorinostat
Sor. + Vor.
GFP-LC3 + JNK-IP
P-PERK
P-JNK
GAPDH
VEH
Sor.+Vor.
VEH
Sor.+Vor.
siSCR
siCD95

Walker et al., Figure 5C

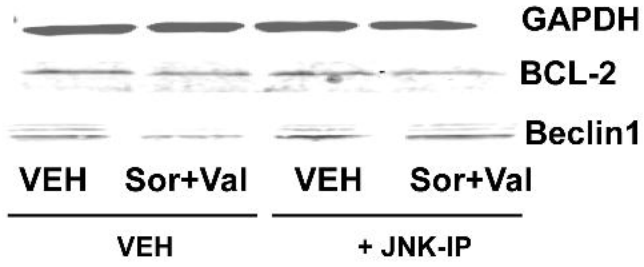

Figure 6A

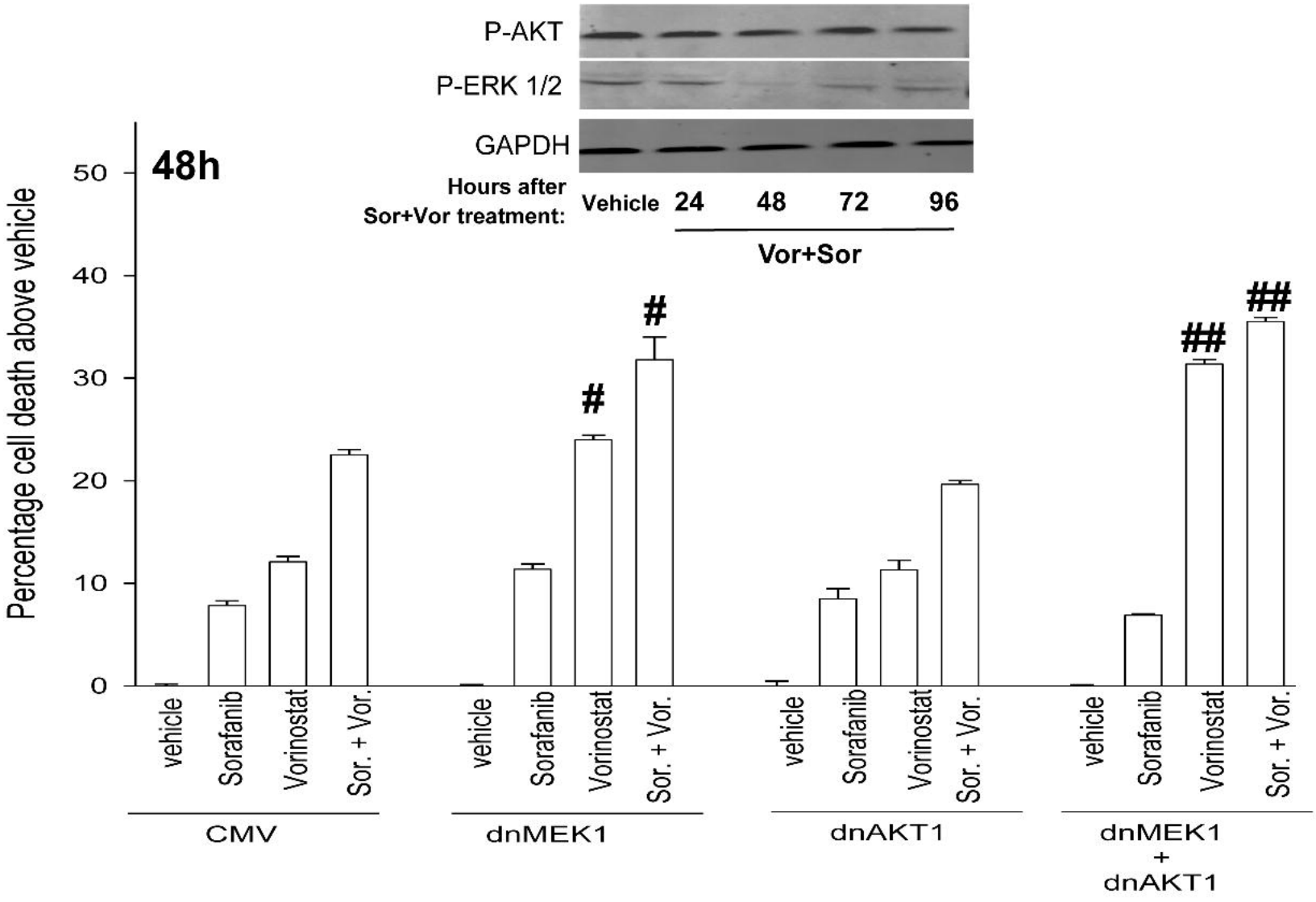
P-AKT
P-ERK 1/2
GAPDH
Hours after Sor+Vor treatment:
Vehicle
24
48
72
96
Vor+Sor
48h
Percentage cell death above vehicle
0
10
20
30
40
50
#
#
##
##
vehicle
Sorafanib
Vorinostat
Sor. + Vor.
CMV
dnMEK1
dnAKT1
dnMEK1 + dnAKT1

Figure 6B

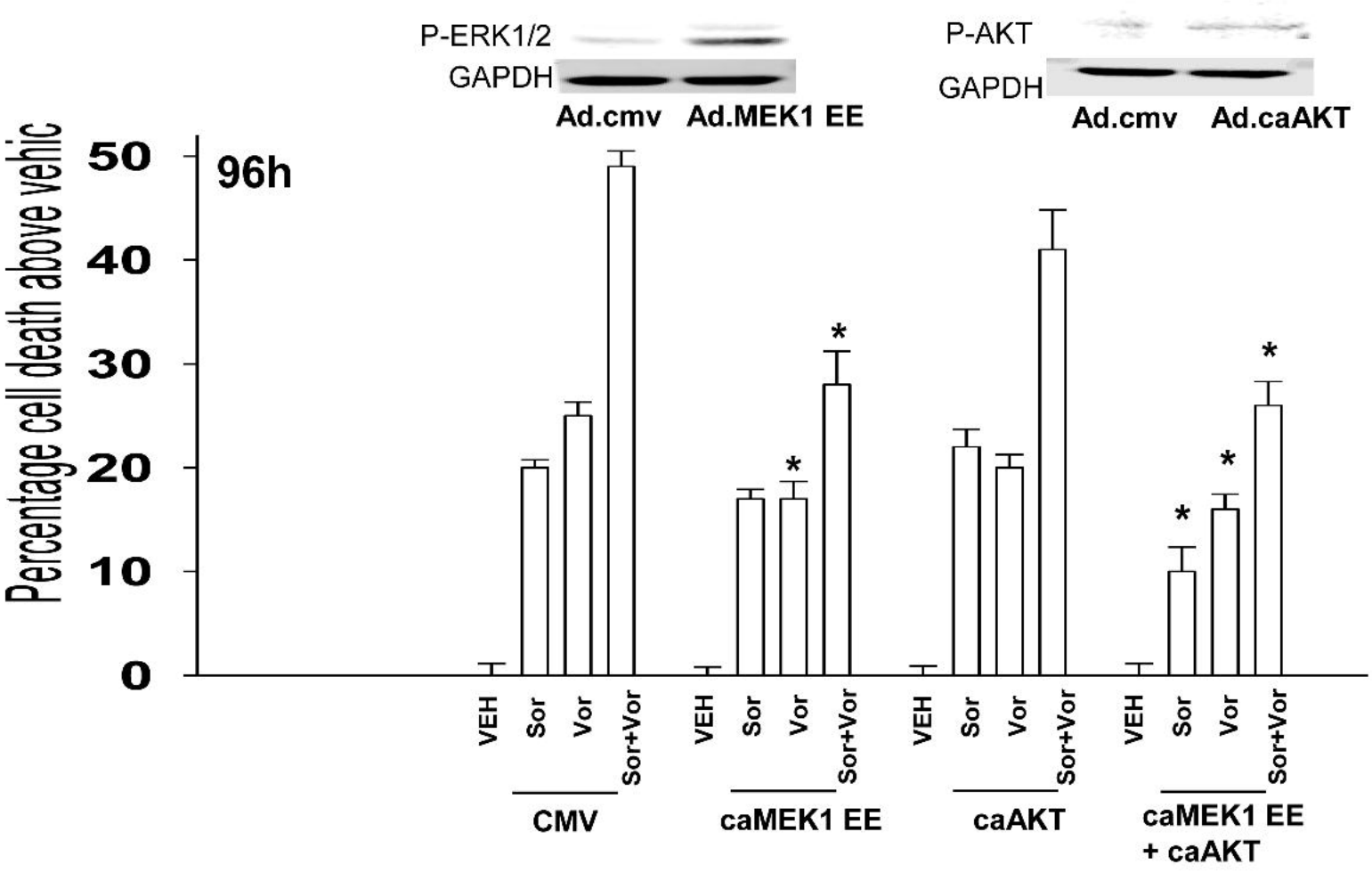
P-ERK1/2
GAPDH
Ad.cmv
Ad.MEK1 EE
P-AKT
GAPDH
Ad.cmv
Ad.caAKT
96h
Percentage cell death above vehic
50
40
30
20
10
0
VEH
Sor
Vor
Sor+Vor
CMV
caMEK1 EE
caAKT
caMEK1 EE
+ caAKT